UNCERTAIN LINEAR EQUATIONS

A THESIS

SUBMITTED TO THE DEPARTMENT OF ELECTRICAL AND

ELECTRONICS ENGINEERING

AND THE INSTITUTE OF ENGINEERING AND SCIENCES

OF BILKENT UNIVERSITY

IN PARTIAL FULFILLMENT OF THE REQUIREMENTS

FOR THE DEGREE OF

MASTER OF SCIENCE

By

Mert Pilancı

July 2010

I certify that I have read this thesis and that in my opinion it is fully adequate, in scope and in quality, as a thesis for the degree of Master of Science.

Prof. Dr. Orhan Arıkan (Supervisor)

I certify that I have read this thesis and that in my opinion it is fully adequate, in scope and in quality, as a thesis for the degree of Master of Science.

Prof. Dr. Erdal Arıkan

I certify that I have read this thesis and that in my opinion it is fully adequate, in scope and in quality, as a thesis for the degree of Master of Science.

Prof. Dr. Mustafa Ç. Pınar

Approved for the Institute of Engineering and Sciences:

Prof. Dr. Levent Onural
Director of Institute of Engineering and Sciences

ABSTRACT

UNCERTAIN LINEAR EQUATIONS

Mert Pilancı
M.S. in Electrical and Electronics Engineering
Supervisor: Prof. Dr. Orhan Arıkan
July 2010

In this thesis, new theoretical and practical results on linear equations with various types of uncertainties and their applications are presented. In the first part, the case in which there are more equations than unknowns (overdetermined case) is considered. A novel approach is proposed to provide robust and accurate estimates of the solution of the linear equations when both the measurement vector and the coefficient matrix are subject to uncertainty. A new analytic formulation is developed in terms of the gradient flow to analyze and provide estimates to the solution. The presented analysis enables us to study and compare existing methods in literature. We derive theoretical bounds for the performance of our estimator and show that if the signal-to-noise ratio is low than a treshold, a significant improvement is made compared to the conventional estimator. Numerical results in applications such as blind identification, multiple frequency estimation and deconvolution show that the proposed technique outperforms alternative methods in mean-squared error for a significant range of signal-to-noise ratio values. The second type of uncertainty analyzed in the overdetermined case is where uncertainty is sparse in some basis. We show that this type of uncertainty on the coefficient matrix can be recovered exactly for a large class of structures, if we have sufficiently many equations. We propose and solve an optimization

criterion and its convex relaxation to recover the uncertainty and the solution to the linear system. We derive sufficiency conditions for exact and stable recovery. Then we demonstrate with numerical examples that the proposed method is able to recover unknowns exactly with high probability. The performance of the proposed technique is compared in estimation and tracking of sparse multipath wireless channels. The second part of the thesis deals with the case where there are more unknowns than equations (underdetermined case). We extend the theory of polarization of Arikan for random variables with continuous distributions. We show that the Hadamard Transform and the Discrete Fourier Transform, polarizes the information content of independent identically distributed copies of *compressible* random variables, where compressibility is measured by Shannon's differential entropy. Using these results we show that, the solution of the linear system can be recovered even if there are more unknowns than equations if the number of equations is sufficient to capture the entropy of the uncertainty. This approach is applied to sampling compressible signals below the Nyquist rate and coined "Polar Sampling". This result generalizes and unifies the sparse recovery theory of Compressed Sensing by extending it to general low entropy signals with an information theoretical analysis. We demonstrate the effectiveness of Polar Sampling approach on a numerical sub-Nyquist sampling example.

Keywords: Statistical Signal Processing, Linear Algebra, Least Squares Estimation, Errors in Variables Model, Sparse Signal Processing, Compressed Sensing, Information Theory, Polar Codes, Source Polarization

ÖZET

BELİRSİZ DENKLEM SİSTEMLERİ

Mert Pilancı
Elektrik ve Elektronik Mühendisliği Bölümü Yüksek Lisans
Tez Yöneticisi: Prof. Dr. Orhan Arıkan
Temmuz 2010

Bu tezde, çeşitli belirsizlikler içeren denklem sistemleri için kuramsal sonuçlar ve uygulamaları sunulmaktadır. İlk kısımda, denklem sayısının bilinmeyen sayısından fazla olduğu durum (artık belirtilmiş) ele alınmaktadır. Katsayı matrisi ve ölçüm vektöründe birlikte belirsizlik bulunan denklem sistemleri için gürbüz ve isabetli yeni bir yöntem önerilmektedir. Çözüme ulaşmak ve başarımı analiz etmek için gradyan alanına dayalı yeni bir analitik yaklaşım sunulmaktadır. Sunulan kuramsal sonuçlar literatürde bilinen diğer yöntemlerin de incelenmesi için kullanılmıştır. Önerilen yöntem için başarım sınırları türetilmiş ve sinyal gürültü oranının belirli bir miktardan düşük olduğu durumda önerilen yöntemin diğer yöntemlere kıyasla daha başarılı olduğu ispatlanmıştır. Sayısal sonuçlar kısmında sistem tanımlama, çoklu frekans kestirimi ve ters evrişim problemlerindeki başarım oranı diğer yöntemlerle karşılaştırılmış ve düşük sinyal gürültü oranları için daha az toplam hata kare elde edilmiştir. Bu bölümde incelenen diğer bir belirsizlik modeli de seyrek belirsizliktir. Bu tür belirsizliklerin eğer yeteri kadar denklem varsa bazı koşullar altında kesin olarak çözülebileceği gösterilmiştir. Çözüm için bir optimizasyon kriteri ve konveks relaksiyonu önerilmektedir. Kesin ve kararlı çözüm için yeterli koşullar bulunmuştur. Nümerik örnekler önerilen yöntemin kesin çözüm olasılığının yüksek

olduğunu göstermektedir. Yöntem kablosuz çokyollu kanal kestirim ve takibine uygulanmış ve yüksek başarım sağlanmıştır. Tezin ikinci kısmında bilinmeyen sayısı denklem sayısından fazla olduğu (eksik belirtilmiş) durum ele alınmıştır. Arıkan'ın kutuplaşma kuramı sürekli dağılımlı rastgele değişkenlere genişletilerek, Hadamard ve Ayrık Fourier Dönüşümü'nün bağımsız eş dağılımlı sıkıştırılabilir değişkenlerdeki bilgi içeriğini kutuplaştırdığı gösterilmiştir. Elde edilen bu sonuçlarla, eğer gözlem entropisi yeterliyse doğrusal denklem sistemin çözümünün belirlenebileceği gösterilmiştir. Bu yaklaşım sıkıştırılabilir sinyalleri örneklemeye uygulanmış ve "Kutupsal Örnekleme" adı verilmiştir. Bu sonuç Sıkıştırmalı Örnekleme (Compressive Sampling) kuramının seyrek sinyallerden sıkıştırılabilir sinyallere bilgi kuramı yardımıyla genellenmesini sağlamıştır. Kutupsal Örnekleme yöntemi sayısal olarak dalgacıklar yardımıyla sıkıştırılabilir bir sinyali Nyquist hızı altında örneklemede denenmiş ve sonuçlar sunulmuştur.

Anahtar Kelimeler: İstatistiksel Sinyal İşleme, Doğrusal Cebir, En Az Kareler, Toplam En Az Kareler, Seyrek Sinyal İşleme, Sıkıştırmalı Örnekleme, Bilgi Kuramı, Kutuplaşma Kodları, Kaynak Kutuplaşması.

Contents

List of Figures

List of Tables

Dedicated to my family

Chapter 1

INTRODUCTION

The subject of this thesis is the recovery of uncertainty in linear equations. The work can be divided basically into two parts: *The Overdetermined Case*, where the number of equations exceeds the number of unknowns and *The Underdetermined Case*, which is the exact opposite. In the first part we develop theoretical notions to analyze various forms of matrix uncertainty for overdetermined linear equations. Then we propose new estimators to cope with the uncertainty and derive bounds for their performance. The main result of the first part is that, since we have more equations than unknowns, the uncertainty (and consequently the unknowns of the linear equation) can be recovered statistically or exactly depending on the structure of the uncertainty. The second part deals with the underdetermined case. Following the work of Arikan, we develop the theory of information polarization for random variables with continuos distributions. Then we prove that using a specially structured matrix, it is possible to recover the unknowns using few equations.

1.2 Overdetermined Linear Equations

In various signal processing applications including deconvolution, signal modeling, frequency estimation, blind channel identification and equalization, it is important to produce robust estimates for an unknown vector $\mathbf{x}$ from a set of measurements $\mathbf{y}$. Typically, a linear model is used to relate the unknowns to the available measurements: $\mathbf{y} = \mathbf{A}\mathbf{x} + \mathbf{w}$, where the matrix $\mathbf{A} \in \mathbb{R}^{m \times n}$ describes the linear relationship and $\mathbf{w}$ is additive measurement noise. Over the years, a multitude of techniques have been developed to obtain better estimates for $\mathbf{x}$. For instance, if $\mathbf{x}$ is a random vector with known first and second order statistics, the Wiener estimator, which minimizes the mean-squared error (MSE) over all linear estimators, can be used with proven success [1]. In the absence of such a statistical information on $\mathbf{x}$, the Least Squares (LS) criterion is commonly used when the number of equations exceeds the number of unknowns. The well known LS method for solving the overdetermined linear equations $\mathbf{A}\mathbf{x} = \mathbf{y}$ for $m > n$, yields the Maximum Likelihood (ML) estimate of the deterministic unknown $\mathbf{x}$ when the observations are subject to independent identically distributed (i.i.d.) Gaussian noise and has the minimum MSE over all unbiased estimators [2]. In practice, the observation $\mathbf{y}$ is noisy and the elements of matrix $\mathbf{A}$ are also subject to errors since they may be results of some other measurements or obtained under some modeling assumptions. When the errors in $\mathbf{A}$ and $\mathbf{y}$ are zero mean i.i.d. Gaussian random variables, the ML estimate can be obtained by the Total Least Squares (TLS) technique, which "corrects" the system with minimum perturbation so that it becomes consistent [3, 4]. However in many applications, the linear system of equations has a structure, e.g., Toeplitz, Hankel, Vandermonde, hence the i.i.d. assumption on the errors is not valid. For that reason, the Structured Total Least Squares (STLS) techniques and its regularized versions (RSTLS) have been developed to obtain an accurate estimate by employing

minimal norm structured perturbations on the original system until consistency is reached [5–7].

In two alternative Min-Max optimal approaches, the estimator that minimizes the worst case MSE: $E[\|\mathbf{x}-\mathbf{x}_0\|]$, [8, 9] or residual: $\|\mathbf{A}\mathbf{x}-\mathbf{y}\|$, [10] is sought respectively. Min-Max approaches reduce to convex optimization problems. However, the worst case residual approach which is known as Structured Robust Least Squares (SRLS), can also be applied to any linear structured uncertainty. Furthermore, the SRLS problem can be efficiently solved using second order cone programming [11]. The solution can be interpreted as a Tikhonov regularization in the unstructured case [12, 13]. When $\mathbf{A}$ is ill-conditioned, the Min-Max solution produces a biased $\hat{\mathbf{x}}$ to avoid the residual norm becoming unacceptably large. As a result the Min-Max approach may be overly conservative and its average performance is usually undesirable in many applications. Furthermore, the performance of the Min-Max techniques varies significantly based on the uncertainty bounds that might not be readily available.

For overdetermined linear equations, we propose and analyze a new method, Structured Least Squares with Bounded Data Uncertainties (SLS-BDU), to provide a better trade-off between the accuracy and robustness of the estimates for the solution to $\mathbf{A}\mathbf{x}=\mathbf{y}$ under structured and bounded uncertainty in $\mathbf{A}$ and $\mathbf{y}$. Unlike the SRLS technique that minimizes the worst case error, the proposed SLS-BDU technique minimizes the best case residual. For ill-conditioned problems, it is demonstrated both in theory and simulations that a small norm bound on the perturbation regularizes the solution and prevents numerical instability which is usually exhibited by the STLS estimator. The proposed estimator does not force the consistency of given equations, which is the primary reason of instability in practice. Instead, the most likely solution that is within the confidence bounds of the perturbations is found. There are important signal processing applications where such bounds on the perturbations are known. Hence, the

proposed approach is well suited for such applications including array signal processing, channel estimation [14] and equalization [15], system identification [16], spectral estimation [17], signal modeling [18] where STLS is readily applied. When bounds on the perturbations are not available, the bound can be treated as a regularization parameter. For this case, we propose a simple strategy to determine the value of the bound that yields accurate and robust estimates.

The analysis of known estimators and solution of the proposed formulation relies mostly on the Fréchet derivatives of pseudoinverses which was studied in numerical optimization for nonlinear least squares fitting [19]. The geometry of gradient flow of the cost function reveals how the known techniques behave differently and their respective performance over different scenarios. The discussion on the gradient flow leads to a version of SLS-BDU that automatically chooses the bound parameter when it is not available to us. It is shown in numerical examples that the proposed estimator achieves smaller MSE than other alternatives for a large set of SNR values.

1.3 Underdetermined Linear Equations

Although most of the equation systems faced in reality contain far more unknown variables than known quantities, it was long believed that for a reliable solution of a linear system, the number of equations must be at least the number of unknowns. However, recent progress showed that, underdetermined equations can also be solved exactly with very high probability provided that the solution is sparse and the coefficient matrix satisfies certain properties. The first implication of this result was on sampling theory, as it implies sampling and exact recovery below conventional rates. This result is known as *Compressed Sensing* and makes the sub-Nyquist sampling and recovery possible by a dramatic change of

the sensory equipment. In this part of the thesis, we generalize the sparse recovery theory of Compressed Sensing by extending it to general low entropy signals with an information theoretical analysis. We use a specific structured matrix which mimics the source/channel polarization phenomenon of Arikan for random variables with continuous distributions. Using results from Central Limit Theorem and Martingale theory, we show that for compressible signals, few inner products suffice to unveil the uncertainty. Therefore the solvability of the underdetermined system depends on the entropy of the unknowns. This approach was coined "Polar Sampling" when applied to sampling low entropy signals. Although our results are valid for restricted family of matrices including Hadamard and Discrete Fourier matrices, the theoretical methods used in this section can also be used to analyze many other matrix structures and solvability of such underdetermined systems as well. We demonstrate the effectiveness of our Polar Sampling approach on sampling an infinite bandwidth signal below the Nyquist rate.

Chapter 2

UNCERTAIN LINEAR EQUATIONS: Overdetermined Case

2.1 Preliminaries and Notation

Throughout the thesis, we denote by $\mathbf{A}^T$ and $\mathbf{A}^\dagger$ the transpose and Moore-Penrose pseudoinverse of the matrix $\mathbf{A}$ respectively. $\|\mathbf{A}\|_2$ is the spectral norm of $\mathbf{A}$, i.e., the largest singular value and $\sigma_{min}(\mathbf{A})$ is the minimum singular value. For an integer i, $1 \leq i \leq \text{Rank}(\mathbf{A})$, $\sigma_i(\mathbf{A})$ is the i'th largest singular value. $\|\mathbf{A}\|_F \triangleq \sqrt{\sum_i \sigma_i^2(\mathbf{A})}$ denotes the Frobenious norm of $\mathbf{A}$. $\mathbf{A} \odot \mathbf{B}$ denotes the Hadamard, i.e., elementwise product of two matrices of the same size. ∇ and $\mathbf{D}$ are the gradient and Fréchet derivative operators respectively. E denotes expectation of a random variable. $(\cdot)_+$ denotes the positive part of a real scalar and $(\cdot)_i$ denotes the i^{th} sub-array of an array of numbers.

2.2 Review of Existing Approaches

In this section, we provide a short review of algorithms that have been proposed for overdetermined linear system of equations with uncertainties in all variables. The following approaches can be first divided in to two categories, namely the structured and unstructured uncertainties (perturbations on the matrix). The Total Least Squares (TLS) and Unstructured Bounded Errors in Variables approaches are in the first category. The Structured Total Least Squares approach is proposed to fulfill the goals of TLS in case of an existing structure. The Structured Robust Least Squares approach has been proposed to provide Min-Max optimal robust solutions to structured least squares problems. In the following each approach will be briefly reviewed.

2.2.1 The Method of Least Squares

For an overdetermined linear system of equations $\mathbf{A}\mathbf{x} \approx \mathbf{y}$, the well known Least Squares approach assumes that the only uncertainty is on the observations $\mathbf{y}$. And it minimizes the residual,

$$\mathbf{x}_{LS} = \arg\min_{\mathbf{x}} \|\mathbf{A}\mathbf{x} - \mathbf{y}\|_2^2, \tag{2.1}$$

which has the closed form solution,

$$\mathbf{x}_{LS} = (\mathbf{A}^T\mathbf{A})^{-1}\mathbf{A}^T\mathbf{y} = \mathbf{A}^\dagger\mathbf{y}, \tag{2.2}$$

if $\mathbf{A}$ has full column rank. Finding a Least Squares solution can also be seen as finding a minimum norm perturbation $\mathbf{e}$ on the observation $\mathbf{y}$, such that the perturbed system $\mathbf{A}\mathbf{x} = \mathbf{y} + \mathbf{e}$ is consistent.

2.2.2 The Total Least Squares Approach

In reality, the uncertainty is usually not restricted to only $\mathbf{y}$. In Total Least Squares (TLS) approach, it is assumed that the coefficient matrix is also uncertain. In this case, the minimum norm perturbation $[\mathbf{\Delta A}\ \mathbf{\Delta y}]$ on $[\mathbf{A}\ \mathbf{y}]$ that results in a consistent system $(\mathbf{A}+\mathbf{\Delta A})\mathbf{x} = \mathbf{y}+\mathbf{\Delta y}$ is found. The TLS problem can be solved by using the Singular Value Decomposition (SVD) as [3]:

$$\mathbf{x}_{TLS} = (\mathbf{A}^T\mathbf{A} - \sigma_{n+1}^2\mathbf{I})^{-1}\mathbf{A}^T\mathbf{y} \quad , \tag{2.3}$$

where σ_{n+1} is the smallest singular value of $[\mathbf{A}\ \mathbf{y}]$. However, the subtraction of $\sigma_{n+1}^2\mathbf{I}$ from the diagonal of $\mathbf{A}^T\mathbf{A}$ deregulates the inverse operation, hence, results in an increased sensitivity to noise. It is known that the variance of the TLS estimator is always higher than that of the ordinary Least Squares estimator, and increases with the condition number of the true matrix $\mathbf{A}_0$ [20]. A weighted TLS solution provides the ML estimate for the random Gaussian linear model [4]. See [21] for other generalizations of the TLS.

2.2.3 (Regularized) Structured Total Least Squares Approach

Often the imprecisions on $\mathbf{A}$ and $\mathbf{y}$ have a structure that is desired to be kept intact during the perturbations to obtain a consistent system. For this purpose, the structured TLS (STLS) approaches have been proposed as a constrained optimization problem [5], [6], [22]:

$$\begin{gathered}\min_{\mathbf{\Delta A},\mathbf{\Delta y},\mathbf{x}} \|[\mathbf{\Delta A}\ \mathbf{\Delta y}]\|_F + \mu\,\|\mathbf{W}\mathbf{x}\|_2 \\ \text{s.t.}(\mathbf{A}+\mathbf{\Delta A})x = \mathbf{y}+\mathbf{\Delta y} \text{ and} \\ [\mathbf{\Delta A}\ \mathbf{\Delta y}] \text{ has the same structure as } [\mathbf{A}\ \mathbf{y}] \quad ,\end{gathered}$$

where, for $\mu \geq 0$, $\mu \|\mathbf{Wx}\|$ is a penalty term that is used to regularize the solution. If the perturbations are such that the columns of $[\mathbf{\Delta A}\ \mathbf{\Delta y}]$ can be written as,

$$[\mathbf{\Delta A}\ \mathbf{\Delta y}]_i = \mathbf{G}_i \mathbf{v}, \qquad i = 1, ..., n+1 \quad , \tag{2.4}$$

where $\mathbf{v}$ is a white noise vector with variance σ^2, the RSTLS optimization can be reduced to the following nonlinear minimization [23, 24] :

$$\begin{pmatrix} \mathbf{x} \\ -1 \end{pmatrix}^T [\mathbf{A}\ \mathbf{y}]^T (\mathbf{H}_\mathbf{x} \mathbf{H}_\mathbf{x}^T)^{-1} [\mathbf{A}\ \mathbf{y}] \begin{pmatrix} \mathbf{x} \\ -1 \end{pmatrix} + \mu \|\mathbf{Wx}\|_2 \quad , \tag{2.5}$$

where

$$\mathbf{H}_x = \left(\sum_{i=1}^{m} \mathbf{x}_i \mathbf{G}_i \right) - \mathbf{G}_{m+1} \quad . \tag{2.6}$$

Except for block circulant matrices [22], this optimization problem is non-convex and the developed solution techniques are based on local optimization. In [24], it is shown that for high SNR the covariance matrix of the STLS ($\mu = 0$) estimator can be approximated by

$$E[(\hat{\mathbf{x}} - \mathbf{x})(\hat{\mathbf{x}} - \mathbf{x})^T] \approx \sigma^2 (\mathbf{A}_0^T (\mathbf{H}_\mathbf{x} \mathbf{H}_\mathbf{x}^T)^{-1} \mathbf{A}_0)^{-1} \quad . \tag{2.7}$$

If $\mathbf{A}_0$ has a large condition number, the variance can be extremely large. It is usually noted in applications that at low SNR, the error variance is even larger than its approximation in (2.7) [25, 26].

2.2.4 Structured Robust Least Squares Approach

As a member of Min-Max class of techniques, the Structured Robust Least Squares (SRLS) estimates $\mathbf{x}$ as the solution to the following optimization problem:

$$\min_{\mathbf{x}} \max_{\|\delta\|_2 \leq \rho} \left\| (\mathbf{A} + \sum_{i=1}^{p} \delta_i \mathbf{A}_i)\mathbf{x} - (\mathbf{y} + \sum_{i=1}^{p} \delta_i \mathbf{y}_i) \right\|_2 \quad . \tag{2.8}$$

SRLS minimizes the worst case residual over a set of perturbations structured with constant matrices $\mathbf{A}_i$ and vectors $\mathbf{y}_i$. As the bound ρ gets larger, the

obtained solutions become more regularized. Hence, the SRLS approach trades accuracy for robustness. Since the Min-Max criterion is convex, the solution to the SRLS problem can be obtained efficiently by using convex, second-order cone programming [10]. There also exists extensions of this approach incorporating quantization uncertainty in $\mathbf{x}$, which is solvable using convex programming [27].

2.2.5 Unstructured Bounded Errors-in-Variables (UBEV) Model

One of the important unstructured techniques is known as the Bounded Errors-in-Variables approach, where the inner maximization of the unstructured robust least squares is replaced with a minimization over the allowed perturbations [28, 29]:

$$\min_{\mathbf{x}} \quad \min_{\substack{\|[\boldsymbol{\Delta}\mathbf{A}]\|_{\mathrm{F}} \leq \eta_A \\ \|[\boldsymbol{\Delta}\mathbf{y}]\|_2 \leq \eta_y}} \quad \|(\mathbf{A}+\boldsymbol{\Delta}\mathbf{A})\mathbf{x} - (\mathbf{y}+\boldsymbol{\Delta}\mathbf{y})\| \quad .$$

As opposed to the cautious approach taken by the Min-Max techniques, this technique has an optimistic approach and searches for the most favorable perturbation in the allowed set of perturbations. In this sense it is closer to the TLS approach, but more robust since it does not pursue the consistency as in TLS resulting in sensitivity issues. However, unlike the Min-Max case, the Min-Min approach may be degenerate if the residual becomes zero [29]. The non-degenerate and unstructured case has the same form as the TLS solution

$$\mathbf{x}_{UBEV} = (\mathbf{A}^{\mathrm{T}}\mathbf{A} - \gamma\mathbf{I})^{-1}\mathbf{A}^{\mathrm{T}}\mathbf{y} \quad ,$$

for some positive valued γ which depends on the perturbation bounds and can be solved using secular equation techniques [30]. For small enough bounds on the perturbations, it can be shown that the value of γ is less than that of σ_{n+1}^2 in the TLS solution given in Eqn. 2.3, resulting in less de-regularization than the TLS, hence more robust solutions.

The Extended Least Squares (XLS) criterion [31], which is a blend of LS and STLS is another technique worth noting. In XLS and similar techniques [32], the model errors and measurement errors are distinguished using a weighted minimization.

2.3 Structured Least Squares with Bounded Data Uncertainties

We will consider the following deterministic relationship between the true variables of a linear system:

$$\mathbf{y}_0 = \mathbf{A}_0\mathbf{x} \quad , \tag{2.9}$$

where the true matrix $\mathbf{A}_0 \in \mathbb{R}^{m\times n}$ maps the unknowns $\mathbf{x}$ to $\mathbf{y}_0$. However neither $\mathbf{A}_0$ nor $\mathbf{y}_0$ is available to us directly. The measured $\mathbf{y}$ is related to $\mathbf{y}_0$ as:

$$\mathbf{y} = \mathbf{y}_0 + \sum_{i=1}^{p} \mathbf{y}_i\theta_i + \mathbf{w} \quad , \tag{2.10}$$

where non-zero values of θ_i cause structured uncertainty and $\mathbf{w}$ is additive i.i.d. noise vector with variance σ_w^2. Furthermore, the observed untrue matrix $\mathbf{A}$ is a structurally perturbed version of $\mathbf{A}_0$:

$$\mathbf{A} = \mathbf{A}_0 + \sum_{i=1}^{p} \mathbf{A}_i\theta_i \quad . \tag{2.11}$$

Here, both $\mathbf{A}_i$ and $\mathbf{y}_i$ are fixed matrices with known structure and θ_i is the i'th element of the perturbation vector $\boldsymbol{\theta}$. Note that the structured errors in $\mathbf{A}$ and $\mathbf{y}$ may be correlated in this setup as in the case of Linear Prediction Equations used in harmonic superresolution, AR and ARMA modeling [24, 33]. In those applications such as deconvolution or system identification where no structure exists in the measurement vector, all $\mathbf{y}_i$'s can be set to zero.

2.3.1 The Proposed Optimization Problem

Borrowing the uncertainty set idea from the Min-Max framework we formulate the following optimization problem that is closer to the Maximum Likelihood solution in spirit,

$$\min_{\mathbf{x}} \min_{\|\mathbf{W}\boldsymbol{\alpha}\|_2 \leq \rho} \left\| (\mathbf{A} + \sum_{i=1}^{p} \alpha_i \mathbf{A}_i)\mathbf{x} - (\mathbf{y} + \sum_{i=1}^{p} \alpha_i \mathbf{y}_i) \right\|_2^2, \tag{2.12}$$

which is a generalization of the Bounded Errors-in-Variables model to the structured case [28]. Here, $\mathbf{W}$ is a positive-definite weighting matrix which may be used to incorporate prior knowledge of perturbations, e.g., imposing frequency domain constraints. Unlike the Min-Max case this optimization problem is non-convex in general. In the following, we consider the cases of deterministic and random perturbations and we will assume that ρ is small enough so that the objective of (2.12) is always positive.

Deterministic Perturbations

In Appendix A, given observations of $\mathbf{y}$ and $\mathbf{A}$, we show that there is no unbiased estimator of $\mathbf{x}$ with finite variance if $p > m - n$. This is because of the fact that for $p > m - n$ the Fisher Information Matrix is singular for a deterministic unknown vector $\boldsymbol{\theta}$. In particular this result applies to commonly encountered Toeplitz and Hankel structures which have $p = m + n - 1$. If the uncertainty bounds of measurements are known beforehand, a reasonable biased estimate can be obtained even though the Cramer-Rao Lower Bound is infinite, by using the proposed constrained optimization. This case is demonstrated in the signal restoration application in Section 2.7 where the impulse response has an uncertainty with known bounds.

Random Perturbations

As a data preprocessing step, if the actual perturbation $\boldsymbol{\theta}$ is modeled as a random vector with non-zero mean $\mathbf{m}_{\boldsymbol{\theta}}$ and positive definite covariance matrix $\boldsymbol{\Sigma}$, one can define a new set of matrices and vectors:

$$\tilde{\mathbf{A}} = \mathbf{A} + \mathbf{m}_{\boldsymbol{\theta}} \sum_{i=1}^{p} \mathbf{A}_i \quad , \qquad \tilde{\mathbf{y}} = \mathbf{y} + \mathbf{m}_{\boldsymbol{\theta}} \sum_{i=1}^{p} \mathbf{y}_i \quad , \tag{2.13}$$

$$\tilde{\mathbf{A}}_j = \sum_{i=1}^{p} P_{ij} \mathbf{A}_i \quad , \qquad \tilde{\mathbf{y}}_j = \sum_{i=1}^{p} P_{ij} \mathbf{y}_i \quad , \tag{2.14}$$

where $\mathbf{P}$ is the Cholesky factor of the covariance matrix, $\boldsymbol{\Sigma} = \mathbf{P}\mathbf{P}^T$. These new set of matrices enable us to use a whitened perturbation vector. Hence, without loss of generality, we can assume $\boldsymbol{\theta}$ is a zero mean random vector containing independent identically distributed elements with variance σ^2. Then we have the expectation:

$$E[\mathbf{A}^T\mathbf{A}] = \mathbf{A}_0^T\mathbf{A}_0 + \sum_i \sum_j \mathbf{A}_i^T\mathbf{A}_j E[\boldsymbol{\theta}_i\boldsymbol{\theta}_j] \tag{2.15}$$

$$= \mathbf{A}_0^T\mathbf{A}_0 + \sigma^2 \sum_i \mathbf{A}_i^T\mathbf{A}_i \quad . \tag{2.16}$$

For Toeplitz or Hankel structures, this expression can be further simplified to:

$$E[\mathbf{A}^T\mathbf{A}] = \mathbf{A}_0^T\mathbf{A}_0 + m\sigma^2\mathbf{I} \quad . \tag{2.17}$$

The above expression and also (2.16) illustrate the fact that, as a result of the diagonal loading term, even if $\mathbf{A}_0$ is an ill-conditioned matrix, the observed matrix may be well-conditioned. Hence searching for a consistent system $\mathbf{A}_0\mathbf{x} = \mathbf{y}_0$ by employing perturbations on the observed system $(\mathbf{A}, \mathbf{y})$ could result in an inadmissible estimator with large variance. Adding a regularization term as in the RSTLS formulation may be a remedy for this problem. However as will be shown next, by using the proposed approach defined in (2.12), it is possible to find an estimator with smaller MSE.

2.3.2 The Mean Squared Error of the SLS-BDU Estimate

The proposed estimator falls into the class of biased estimators for the linear model where bias-variance tradeoff is of primary importance [34,35]. To provide further insight, we next derive an MSE bound which indicates a similar tradeoff. We begin with the following definitions:

Definition 1. *For a constant* $\boldsymbol{\alpha} \in \mathbb{R}^p$ *define functions,*

$$\mathbf{A}(\boldsymbol{\alpha}) \triangleq \mathbf{A} + \sum_{i=1}^{p} \alpha_i \mathbf{A}_i \quad , \qquad \mathbf{y}(\boldsymbol{\alpha}) \triangleq \mathbf{y} + \sum_{i=1}^{p} \alpha_i \mathbf{y}_i \quad . \tag{2.18}$$

Without loss of generality we will assume that $\mathbf{y}_i = 0 \ \forall i$ in the rest of the thesis, since they can be embedded into $\tilde{\mathbf{A}}_i \triangleq [\mathbf{A}_i \ \ \mathbf{y}_i]$'s as follows:

$$\mathbf{A}(\boldsymbol{\alpha})\mathbf{x} - \mathbf{y}(\boldsymbol{\alpha}) = \mathbf{A} + \left(\sum_i [\mathbf{A}_i \ \ \mathbf{y}_i] \alpha_i \right) [\mathbf{x} \quad -1]^T - \mathbf{y} \quad . \tag{2.19}$$

Then the following theorem characterizes the MSE of the proposed estimator,

Theorem 2.3.1. *For* $\mathbf{A}(\boldsymbol{\alpha})$ *which is of full column rank for* $\|\mathbf{W}\boldsymbol{\alpha}\|_2 \leq \rho$*, the optimal* $\hat{\mathbf{x}}$ *for the proposed optimization in (2.12) has the following MSE upper bound,*

$$E[\|\hat{\mathbf{x}} - \mathbf{x}\|_2^2] \leq \left(\|\mathbf{x}\|_2^2 \, E \, \|\mathbf{A}(\boldsymbol{\alpha}^*) - \mathbf{A}_0)\|_2^2 + n\sigma_{\mathbf{w}}^2 \right) E[\frac{1}{\sigma_{\boldsymbol{\alpha}^*}^2}] \ ,$$

where $\boldsymbol{\alpha}^*$ *is the optimal* $\boldsymbol{\alpha}$ *of (2.12) and* $\sigma_{\boldsymbol{\alpha}^*}$ *is the minimum singular value of* $\mathbf{A}(\boldsymbol{\alpha}^*)$.

Proof:

By analytically minimizing (2.12) over $\mathbf{x}$ for a fixed $\boldsymbol{\alpha}$ as an ordinary least squares problem, (2.12) reduces to

$$\min_{\|\mathbf{W}\boldsymbol{\alpha}\| \leq \rho} \left\| \mathbf{A}(\boldsymbol{\alpha})\mathbf{A}(\boldsymbol{\alpha})^\dagger \mathbf{y} - \mathbf{y} \right\|_2^2 = \min_{\|\mathbf{W}\boldsymbol{\alpha}\| \leq \rho} \left\| \mathbf{P}_{\boldsymbol{\alpha}}^{\perp} \mathbf{y} \right\|_2^2 \quad , \tag{2.20}$$

where $\mathbf{P}_{\boldsymbol{\alpha}}^{\perp} \triangleq \mathbf{I} - \mathbf{A}(\boldsymbol{\alpha})\mathbf{A}(\boldsymbol{\alpha})^\dagger$ is the projector matrix of the subspace perpendicular to the Range($\mathbf{A}(\boldsymbol{\alpha})$) and we assumed $\mathbf{A}(\boldsymbol{\alpha})$ is of full column rank for $\|\mathbf{W}\boldsymbol{\alpha}\|_2 \leq$

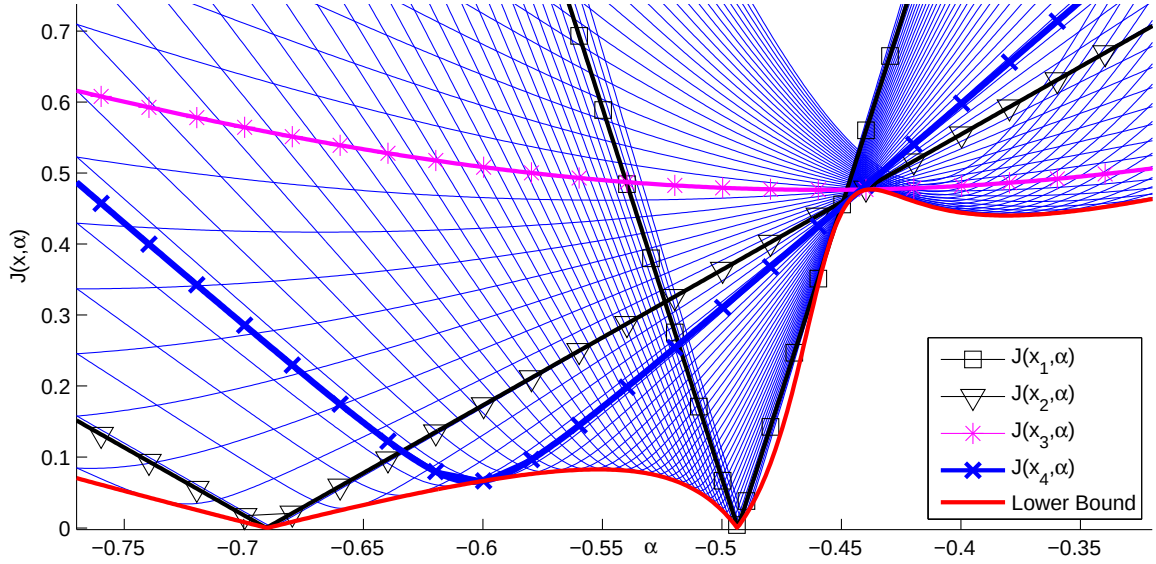

Figure 2.1: Cost $J(\mathbf{x}, \boldsymbol{\alpha})$ in (2.28) plotted for a set of estimators on top of each other.

ρ. Thus, SLS-BDU estimator chooses the $\boldsymbol{\alpha}$ that minimizes the norm of the observation $\mathbf{y}(\boldsymbol{\alpha})$ which lies out of the range of $\mathbf{A}(\boldsymbol{\alpha})$.

The SLS-BDU estimate $\mathbf{x}$ which minimizes (2.12) can be written in terms of the optimal $\boldsymbol{\alpha}^*$ of (2.20) as:

$$\hat{\mathbf{x}}_{SLS-BDU} = \mathbf{A}(\boldsymbol{\alpha}^*)^\dagger \mathbf{y} \quad . \tag{2.21}$$

Since $\mathbf{y} = \mathbf{A}_0\mathbf{x} + \mathbf{w}$, the MSE of (2.21) can be written as [34]:

$$\begin{aligned} E[\|\hat{\mathbf{x}} - \mathbf{x}\|_2^2] &= E[\left\|(\mathbf{A}(\boldsymbol{\alpha}^*)^\dagger \mathbf{A}_0 - \mathbf{I})\mathbf{x} + \mathbf{A}(\boldsymbol{\alpha}^*)^\dagger \mathbf{w}\right\|_2^2] \\ &= E[\left\|(\mathbf{A}(\boldsymbol{\alpha}^*)^\dagger \mathbf{A}_0 - \mathbf{I})\mathbf{x}\right\|_2^2] \\ &\quad + E[\mathrm{Tr}\{\mathbf{A}(\boldsymbol{\alpha}^*)^{\dagger T} \mathbf{A}(\boldsymbol{\alpha}^*)^\dagger \mathbf{w}\mathbf{w}^T\}] \quad . \end{aligned} \tag{2.22}$$

Since, $E[\mathrm{Tr}\{\mathbf{A}(\boldsymbol{\alpha}^*)^{\dagger T} \mathbf{A}(\boldsymbol{\alpha}^*)^\dagger \mathbf{w}\mathbf{w}^T\}] = \sigma_{\mathbf{w}}^2 E[\left\|\mathbf{A}(\boldsymbol{\alpha}^*)^\dagger\right\|_F^2]$, we get:

$$E[\|\hat{\mathbf{x}} - \mathbf{x}\|_2^2] = E\left\|(\mathbf{A}(\boldsymbol{\alpha}^*)^\dagger \mathbf{A}_0 - \mathbf{I})\mathbf{x}\right\|_2^2 + \sigma_{\mathbf{w}}^2 E\left\|\mathbf{A}(\boldsymbol{\alpha}^*)^\dagger\right\|_F^2 . \tag{2.23}$$

The following inequalities that are valid for full column rank matrices $\mathbf{F}$ and $\mathbf{G}$ help to obtain the desired upper bound:

$$\begin{aligned} \left\|\mathbf{F}^{\dagger}\mathbf{G}-\mathbf{I}\right\|_2 = \left\|\mathbf{F}^{\dagger}(\mathbf{G}-\mathbf{F})\right\|_2 &\leq \left\|\mathbf{F}^{\dagger}\right\|_2 \|\mathbf{G}-\mathbf{F}\|_2 , \\ \text{and, } \left\|\mathbf{F}^{\dagger}\right\|_F^2 = \sum_{i=1}^{n} \frac{1}{\sigma_i^2(\mathbf{F})} &\leq \frac{n}{\sigma_{min}^2(\mathbf{F})}. \end{aligned}$$

Using the previous inequality, we can upper bound (2.23) using:

$$\begin{aligned} & E\left[\left\|\mathbf{A}(\boldsymbol{\alpha}^*)^{\dagger}\right\|_2^2 \|\mathbf{A}(\boldsymbol{\alpha}^*)-\mathbf{A}_0\|_2^2 \|\mathbf{x}\|_2^2\right] + E\left[\sum_{i=1}^{n} \frac{\sigma_{\mathbf{w}}^2}{\sigma_{\boldsymbol{\alpha}^*,i}^2}\right] \\ & \leq \left(\|\mathbf{x}\|_2^2 E\|\mathbf{A}(\boldsymbol{\alpha}^*)-\mathbf{A}_0)\|_2^2 + n\sigma_{\mathbf{w}}^2\right) E[\frac{1}{\sigma_{\boldsymbol{\alpha}^*}^2}] \quad . \end{aligned}$$

The obtained upper bound clearly shows that the MSE of the estimate has two parts: the part that increase with the difference between $\mathbf{A}_0$ and its estimate $\mathbf{A}(\alpha^*)$ and the part that increases with the Frobenious norm of the $\mathbf{A}^{\dagger}(\alpha^*)$. Since the Frobenious norm of $\mathbf{A}^{\dagger}(\alpha^*)$ can be very large for an ill conditioned $\mathbf{A}_0$ when the estimate $\mathbf{A}(\alpha^*)$ gets close to $\mathbf{A}_0$, the second part of the bound can get extremely large. Therefore the main idea behind the proposed estimator is to bound the allowed perturbations such that the MSE in (2.23) is near optimal. It is straightforward to show that when $\rho = 0$, the SLS-BDU solution is equal to the ordinary Least Squares solution. Since the STLS optimization seeks a minimal norm perturbation to zero out the cost function in (2.12), the solution given by STLS is identical to the SLS-BDU solution for a large enough value of the perturbation magnitude bound ρ. However that choice of ρ usually results a large MSE in (2.23) as previously noted in numerical results of [31].

2.3.3 MSE Comparison of SLS-BDU and STLS

Using the MSE bound in (2.3.1) we derive the condition in which the proposed estimator has smaller MSE then the Maximum Likelihood STLS estimator and interpret the result.

Theorem 2.3.2. *For deterministic and bounded perturbations $\boldsymbol{\theta}$, let σ_A and σ_0 be the minimum singular values of $\mathbf{A}$ and $\mathbf{A}_0$ respectively and define:*

$$S \triangleq \begin{cases} \sqrt{p}\max_i \|A_i\|_2 & \textit{Arbitrary structure} \\ \max_i \|A_i\|_F & \textit{Non-overlapping structure} \\ \sqrt{n} & \textit{Toeplitz or Hankel.} \end{cases} \tag{2.24}$$

If the following holds:

$$(\rho + \|\theta\|)^2 S^2 \frac{\|\mathbf{x}_0\|_2^2}{n\sigma_w^2} + 1 \leq \left(\frac{\sigma_A - \rho S}{\sigma_0}\right)_+^2 , \tag{2.25}$$

then the asymptotically MSE of SLS-BDU with weight $\mathbf{W} = \mathbf{I}$, is strictly smaller than STLS.

Proof: See Appendix B.

Remark 1. *Note that the expression $R \triangleq \frac{\|\mathbf{x}_0\|_2^2}{n\sigma_w^2}$ in (2.25) denotes the signal to noise ratio, e.g., if $\mathbf{x}_0$ were a zero mean Gaussian vector with variance σ_x^2, then $E[R] = \sigma_x^2/\sigma_w^2$.*

Remark 2. *The right-hand side of (2.25) is expected to be larger than 1 since, $\sigma_A \gg \sigma_0$ by the observation in equation (2.17).*

Therefore, Theorem 2.3.2 asserts that, when SNR is sufficiently low, the condition in (2.25) is satisfied and the proposed SLS-BDU has smaller error than STLS. Furthermore, for ill conditioned problems where σ_0 is small, the condition (2.25) may hold also for large SNR values. In section 2.7 we show that this theoretical result is in good agreement with numerical experiments.

2.4 Analysis of Estimator Performance in an Illustrative Example

Consider the single parameter equation $\mathbf{A}(\alpha)x = \mathbf{y}(\alpha)$ below:

$$\begin{bmatrix} a_1 + \alpha \\ a_2 \end{bmatrix} x = \begin{bmatrix} y_1 \\ y_2 - \alpha \end{bmatrix} \quad . \tag{2.26}$$

The corresponding structures are:

$$\mathbf{A}_1 = [1 \quad 0]^T \quad , \mathbf{y}_1 = [0 \quad -1]^T \quad , \tag{2.27}$$

Define the cost of x given α by:

$$J(x, \alpha) \triangleq \|\mathbf{A}(\alpha)x - \mathbf{y}(\alpha)\|_2^2 \quad , \tag{2.28}$$

which corresponds to a constant multiple of the negative log-likelihood given α for the observation $\mathbf{y}(\alpha) = \mathbf{A}(\alpha)\mathbf{x} + \mathbf{w}$ where $\mathbf{w}$ is a zero mean Gaussian random variable. Figure 2.1 depicts $J(x, \alpha)$ for several values of x plotted on top of each other for $\{a_1, a_2, y_1, y_2\} = \{0.46, 0.023, 0.38, -0.73\}$. The lower bound achievable for any $\mathbf{x}$ is given by:

$$\min_x \|\mathbf{A}(\alpha)x - \mathbf{y}(\alpha)\|_2^2 = \left\|\mathbf{P}_{\boldsymbol{\alpha}}^{\perp}\mathbf{y}(\alpha)\right\|_2^2 \quad , \tag{2.29}$$

which can be easily shown to be zero only for at most two values of α given by:

$$\alpha_{1,2} = \frac{y_2 - a_1}{2} \pm \sqrt{(\frac{y_2 - a_1}{2})^2 + a_1 y_2 - a_2 y_1} \quad . \tag{2.30}$$

By carefully inspecting Figure 2.1, the two solutions of (2.30) $\alpha_1 = -0.69$ and $\alpha_2 = -0.49$ yields the following estimates for $\mathbf{x}$:

$$x_1 = \mathbf{A}(\alpha_1)^{\dagger}\mathbf{y}(\alpha_1) = -1.62 \text{ and } x_2 = \mathbf{A}(\alpha_2)^{\dagger}\mathbf{y}(\alpha_2) = -10, \tag{2.31}$$

neither of which is robust since they have steeply rising linear costs for a small change in α. We utilize this observation later in Section VII by using the gradient of the lower bound as a measure of this sensitivity. Note that given any random

or deterministic perturbation α, because of the consistency requirement, STLS and RSTLS methods produce either x_1 or x_2. If the system were consistent originally, i.e., $\mathbf{A}_0\mathbf{x} = \mathbf{y}_0$, the expected MSE and residual of such consistency constrained estimators would be large because of the distance $|x_1 - x_2|$. Note that the residual of x_1 is extremely large if α_2 is the true parameter.

In Figure 2.1, the cost corresponding to a Min-Max solutions $x_3 = 0.75$ is also shown. Although the cost Min-Max solution is less sensitive to the variations in α, its average is considerably large.

However the SLS-BDU solution given by (2.12) achieves the lower bound in (2.29) for some α^*, which corresponds to an inconsistent system $\{\mathbf{A}(\alpha^*), \mathbf{y}(\alpha^*)\}$, but balances robustness and accuracy by abandoning the consistency condition. An example of one such solution is given by $x_4 = -2.73$, which is neither over conservative as the Min-Max solution x_3 or over optimistic as the STLS solution x_1.

2.5 Fréchet Derivatives and Gradient Flow

In this section Fréchet Derivatives are introduced to analyze the gradient of the SLS-BDU cost function in detail. Additionally, some analytical results on the rotation of the gradient around singularities, and the existence of consistencies as hyperplanes are presented.

2.5.1 Differentiation of pseudoinverses and projectors

The $m \times n$ matrix function $\mathbf{A}(\boldsymbol{\alpha}) = \mathbf{A} + \sum_{i=1}^{p} \alpha_i \mathbf{A}_i$ is a mapping between $\mathbb{R}^p$ and the space of linear transformations $\mathcal{L}(\mathbb{R}^n, \mathbb{R}^m)$. Assuming $\mathrm{Rank}(\mathbf{A}(\boldsymbol{\alpha}))$ is constant for $\|\mathbf{W}\boldsymbol{\alpha}\|_2 \leq \rho$, the pseudoinverse $\mathbf{A}(\boldsymbol{\alpha})^\dagger$ and the projector $\mathbf{P}_{\boldsymbol{\alpha}}^{\perp} = \mathbf{I} - \mathbf{A}(\boldsymbol{\alpha})\mathbf{A}(\boldsymbol{\alpha})^\dagger$

are both Fréchet differentiable with respect to $\boldsymbol{\alpha}$ and closed form formulas were derived in [19]. Formalism on Fréchet derivatives can be found in [36]. Here we provide some known facts as well as new results relevant to our application.

Definition 2. *The Fréchet derivative of* $\mathbf{A}(\boldsymbol{\alpha})$ *denoted by* $\mathbf{DA}(\boldsymbol{\alpha})$ *is a tridimensional tensor, formed with* p *matrices of size* $m \times n$ *containing partial derivatives of the elements of* $\mathbf{A}$ *with respect to* α_i*, i.e.,* $[\mathbf{DA}(\boldsymbol{\alpha})]_i \triangleq \frac{\partial}{\partial \alpha_i}\mathbf{A}(\boldsymbol{\alpha})$.

The Fréchet derivative of $\mathbf{P}_{\boldsymbol{\alpha}}^{\perp}$ is given in [19] as:

$$\mathbf{DP}_{\boldsymbol{\alpha}}^{\perp} = -\mathbf{DP}_{\boldsymbol{\alpha}} = -\mathbf{P}_{\boldsymbol{\alpha}}^{\perp}\mathbf{DA}(\boldsymbol{\alpha})\mathbf{A}(\boldsymbol{\alpha})^{\dagger} - (\mathbf{P}_{\boldsymbol{\alpha}}^{\perp}\mathbf{DA}(\boldsymbol{\alpha})\mathbf{A}(\boldsymbol{\alpha})^{\dagger})^{\mathbf{T}}. \tag{2.32}$$

The following lemma characterizes each entry in the gradient vector of the SLS-BDU cost function given in (2.20).

Lemma 2.5.1. *Let* $\mathbf{y}(\boldsymbol{\alpha})^{\perp} \triangleq \mathbf{P}_{\boldsymbol{\alpha}}^{\perp}\mathbf{y}(\boldsymbol{\alpha})$ *and* $\mathbf{x}_{\boldsymbol{\alpha}} \triangleq \mathbf{A}(\boldsymbol{\alpha})^{\dagger}\mathbf{y}(\boldsymbol{\alpha})$ *then,*

$$\frac{1}{2}\frac{\partial}{\partial \alpha_i}\left\|\mathbf{P}_{\boldsymbol{\alpha}}^{\perp}\mathbf{y}(\boldsymbol{\alpha})\right\|_2^2 = \left\langle \mathbf{y}(\boldsymbol{\alpha})^{\perp},\, \mathbf{y}_i - \mathbf{A}_i\mathbf{x}_{\boldsymbol{\alpha}} \right\rangle. \tag{2.33}$$

Proof:

$$\begin{aligned}
\nabla_{\boldsymbol{\alpha}}\left\|\mathbf{P}_{\boldsymbol{\alpha}}^{\perp}\mathbf{y}(\boldsymbol{\alpha})\right\|_2^2 &= \nabla_{\boldsymbol{\alpha}}\mathbf{y}(\boldsymbol{\alpha})^{\mathbf{T}}\mathbf{P}_{\boldsymbol{\alpha}}^{\perp}\mathbf{y}(\boldsymbol{\alpha}) \\
&= \mathbf{Dy}(\boldsymbol{\alpha})^{\mathbf{T}}\mathbf{P}_{\boldsymbol{\alpha}}^{\perp}\mathbf{y}(\boldsymbol{\alpha}) + \mathbf{y}(\boldsymbol{\alpha})^{\mathbf{T}}\mathbf{DP}_{\boldsymbol{\alpha}}^{\perp}\mathbf{y}(\boldsymbol{\alpha}) \\
&+ \mathbf{y}(\boldsymbol{\alpha})^{\mathbf{T}}\mathbf{P}_{\boldsymbol{\alpha}}^{\perp}\mathbf{Dy}(\boldsymbol{\alpha}) \\
&= 2\mathbf{y}(\boldsymbol{\alpha})^{\mathbf{T}}\mathbf{P}_{\boldsymbol{\alpha}}^{\perp}\mathbf{Dy}(\boldsymbol{\alpha}) \\
&- 2\mathbf{y}(\boldsymbol{\alpha})^{\mathbf{T}}\mathbf{P}_{\boldsymbol{\alpha}}^{\perp}\mathbf{DA}(\boldsymbol{\alpha})\mathbf{A}(\boldsymbol{\alpha})^{\dagger}\mathbf{y}(\boldsymbol{\alpha}) \\
&= 2\mathbf{y}(\boldsymbol{\alpha})^{\mathbf{T}}\mathbf{P}_{\boldsymbol{\alpha}}^{\perp}(\mathbf{Dy}(\boldsymbol{\alpha}) - \mathbf{DA}(\boldsymbol{\alpha})\mathbf{A}(\boldsymbol{\alpha})^{\dagger}\mathbf{y}(\boldsymbol{\alpha})) \\
&= 2\left\langle \mathbf{P}_{\boldsymbol{\alpha}}^{\perp}\mathbf{y}(\boldsymbol{\alpha}),\, \mathbf{y}_i - \mathbf{A}_i\mathbf{A}(\boldsymbol{\alpha})^{\dagger}\mathbf{y}(\boldsymbol{\alpha}) \right\rangle,
\end{aligned}$$

since $[\mathbf{DA}(\boldsymbol{\alpha})]_i = \mathbf{A}_i$ and $[\mathbf{Dy}(\boldsymbol{\alpha})]_i = \mathbf{y}_i$.

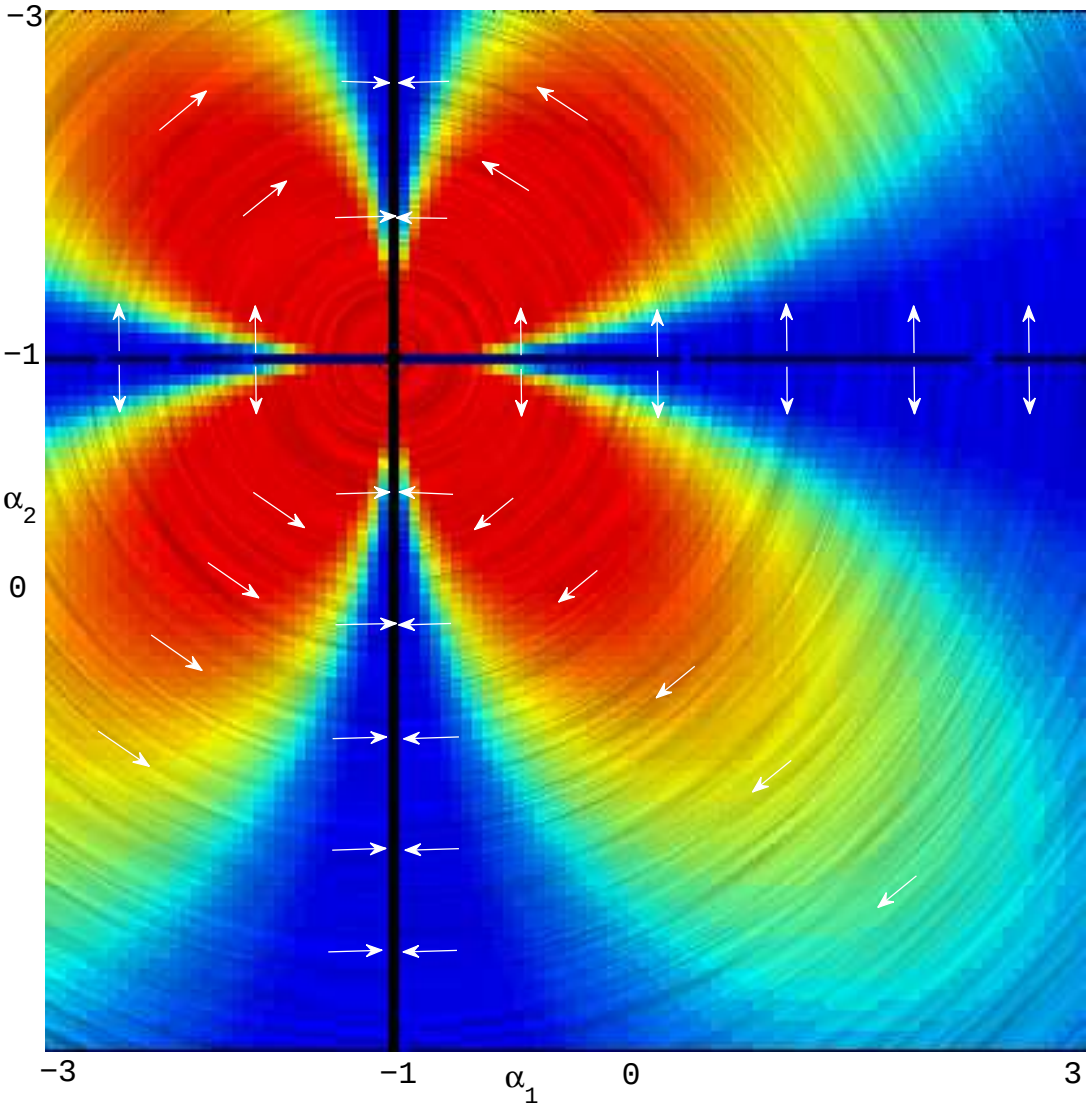

Figure 2.2: Negative gradient field for the two parameter case in (2.34). All vectors rotate around the singularity at $(-1, -1)$.

2.5.2 The Gradient Flow in a Simple Illustrative Case

Consider the following two parameter case:

$$\mathbf{A}(\boldsymbol{\alpha}) = [1+\alpha_1 \;\; 1+\alpha_2]^T \;\;, \quad \mathbf{y}(\boldsymbol{\alpha}) = \mathbf{y} = [0 \;\; 1]^T \;\;, \tag{2.34}$$

which is consistent, i.e., $\mathbf{y}(\boldsymbol{\alpha}) \in \mathrm{R}(\mathbf{A}(\boldsymbol{\alpha}))$ for $\alpha_1 = -1$. The vector field $-\nabla_{\boldsymbol{\alpha}} \left\|\mathbf{P}^{\perp}_{\boldsymbol{\alpha}}\mathbf{y}(\boldsymbol{\alpha})\right\|_2^2$, which is calculated by (3.16) is shown in Figure 2.2. The gradient norm is zero on two straight lines $\boldsymbol{\alpha}_1 = -1$ and $\boldsymbol{\alpha}_2 = -1$ denoting minimum and maximum of (2.20) which intersect at the singular point $(-1,-1)$. The gradient field rotates around the singularity by flowing from the maximum ($\alpha_2 = -1$) to minimum ($\alpha_1 = -1$) and the gradient norm increases gradually as $\boldsymbol{\alpha}$ gets closer to the singular point $(-1,-1)$. In Figure 2.3, the solution of STLS and the proposed solution (2.12) are compared on a diagram for the example in (2.34). The points p_1 and p_2 denote the corrected vectors $\mathbf{A}(\boldsymbol{\alpha})$ for STLS and proposed SLS-BDU for a given ρ and $\mathbf{W} = \mathbf{I}$ respectively. p_1 denotes the closest consistent system while p_2 is the tangent point of the line passing through singularity to the circular boundary with radius ρ. This tangent point geometry was also encountered in unstructured Min-Min and Min-Max problems [30]. It is evident that with a small ρ, the corrected system is better conditioned with the proposed method. Note that for a larger value of ρ, the consistency lines will be in the allowed set of perturbations and the SLS-BDU and the STLS solutions would be identical.

2.5.3 Analytical Results on the Gradient Flow

In this section we present theoretical results which shed light on the interesting geometry of Figure 2.2.

Theorem 2.5.2. *Rotation around a singularity: If Range*$(\mathbf{A}(\boldsymbol{\alpha}_0)) \subset$ *Range*$(\mathbf{A}(\boldsymbol{\alpha}))$*, the gradient field* $\nabla_{\boldsymbol{\alpha}} \left\|\mathbf{P}^{\perp}_{\boldsymbol{\alpha}}\mathbf{y}(\boldsymbol{\alpha})\right\|$ *is orthogonal to* $\boldsymbol{\alpha} - \boldsymbol{\alpha}_0$*, i.e.,*

$$\left\langle \nabla_{\boldsymbol{\alpha}} \left\| \mathbf{P}^{\perp}_{\boldsymbol{\alpha}} \mathbf{y}(\boldsymbol{\alpha}) \right\|_2^2,\ \boldsymbol{\alpha} - \boldsymbol{\alpha}_0 \right\rangle = 0. \tag{2.35}$$

Proof:

By using Lemma 2.5.1 we get,

$$\begin{aligned}
&-\frac{1}{2}\left\langle \nabla_{\boldsymbol{\alpha}} \left\| \mathbf{P}^{\perp}_{\boldsymbol{\alpha}} \mathbf{y}(\boldsymbol{\alpha}) \right\|_2^2,\ \boldsymbol{\alpha}_0 - \boldsymbol{\alpha} \right\rangle \\
&= \sum_i \left\langle \mathbf{P}^{\perp}_{\boldsymbol{\alpha}} \mathbf{y}(\boldsymbol{\alpha}),\ \mathbf{A}_i \mathbf{A}(\boldsymbol{\alpha})^{\dagger} \mathbf{y}(\boldsymbol{\alpha}) \right\rangle (\alpha_i - \alpha_{\mathbf{0}i}) \\
&= \left\langle \mathbf{P}^{\perp}_{\boldsymbol{\alpha}} \mathbf{y}(\boldsymbol{\alpha}),\ \sum_i \mathbf{A}_i [\alpha_{\mathbf{0}i} - \alpha_i] \mathbf{A}(\boldsymbol{\alpha})^{\dagger} \mathbf{y}(\boldsymbol{\alpha}) \right\rangle \\
&= \mathbf{y}(\boldsymbol{\alpha})^{\mathbf{T}} \mathbf{P}^{\perp}_{\boldsymbol{\alpha}} \left[\mathbf{A}(\boldsymbol{\alpha}_{\mathbf{0}}) - \mathbf{A}(\boldsymbol{\alpha}) \right] \mathbf{A}(\boldsymbol{\alpha})^{\dagger} \mathbf{y}(\boldsymbol{\alpha}) \quad .
\end{aligned} \tag{2.36}$$

Because $\text{Range}(\mathbf{A}(\boldsymbol{\alpha}_0)) \subset \text{Range}(\mathbf{A}(\boldsymbol{\alpha}))$ implies $\text{Range}(\mathbf{A}(\boldsymbol{\alpha}_0) - \mathbf{A}(\boldsymbol{\alpha})) \subset \text{Range}(\mathbf{A}(\boldsymbol{\alpha}))$, $\mathbf{P}^{\perp}_{\boldsymbol{\alpha}}(\mathbf{A}(\boldsymbol{\alpha}_0) - \mathbf{A}(\boldsymbol{\alpha})) = \mathbf{0}$, thus (2.36) is zero.

Remark 3. *Theorem 2.5.2 reveals the interesting geometry of Figure 2.2, where all vectors absolutely rotate around the singularity* $(-1, -1)$*, since* $\mathbf{A}(-1, -1)$ *is of rank zero.*

The next theorem states that every singularity is arbitrarily close to a consistency for a range of structures which are commonly encountered in applications.

Theorem 2.5.3. *If there is no structure, or the structure is of Toeplitz or Hankel type, then, for* $\mathbf{A}(\boldsymbol{\alpha})^T \mathbf{A}(\boldsymbol{\alpha})$ *singular, there exists a vector* $\boldsymbol{\epsilon}$ *with arbitrarily small norm, satisfying* $\boldsymbol{k} \in \text{Range}(\mathbf{A}(\boldsymbol{\alpha} + \boldsymbol{\epsilon}))$ *for any arbitrary* $\boldsymbol{k} \in \mathbb{R}^m$*.*

Proof:

First consider the unstructured case and let $\boldsymbol{v} \in \text{Null}(\mathbf{A})$. Then:

$$(\mathbf{A}(\alpha) + \frac{\epsilon}{\boldsymbol{v}^T \boldsymbol{v}} \boldsymbol{k} \boldsymbol{v}^T) \boldsymbol{v} = \epsilon \boldsymbol{k} \tag{2.37}$$

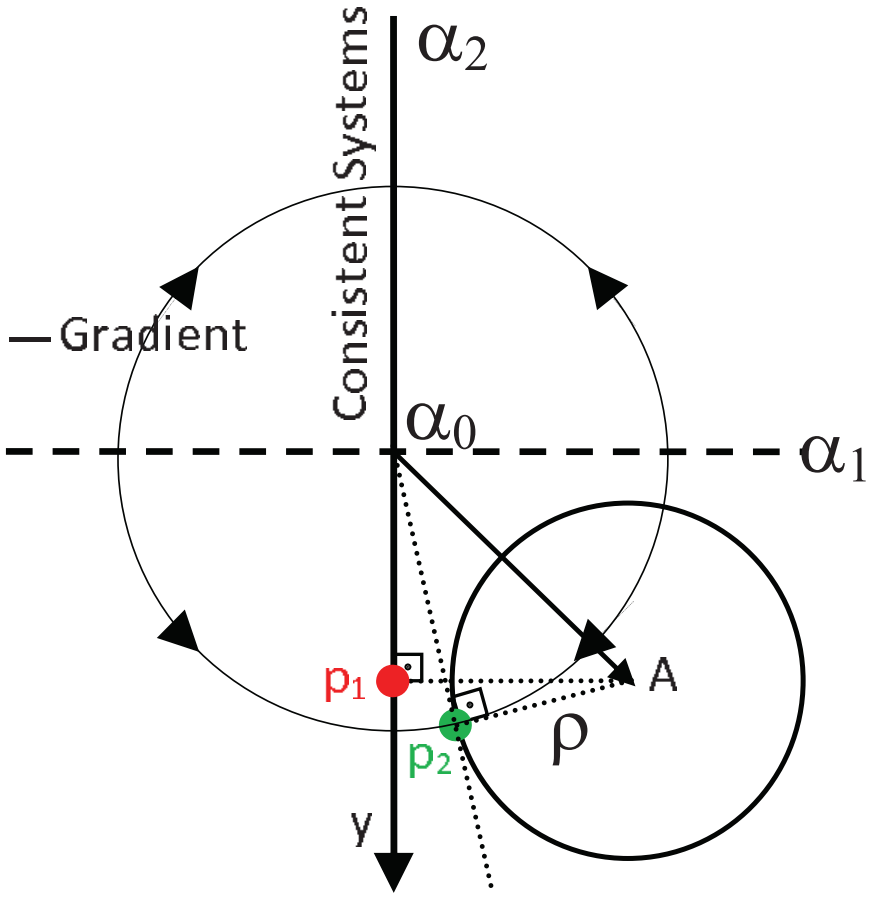

Figure 2.3: Gradient Flow Diagram for the two parameter case in (2.34). The points p_1 and p_2 indicate the perturbations done by STLS and SLS-BDU respectively.

which implies $\boldsymbol{k} \in \text{Range}(\mathbf{A}(\alpha + \boldsymbol{\epsilon}))$. For the Toeplitz case, let $\boldsymbol{v} \in \text{Null}(\mathbf{A}(\boldsymbol{\alpha}))$, then

$$(\mathbf{A}(\boldsymbol{\alpha}) + \sum_i \theta_\mathbf{i} \mathbf{A}_i)\mathbf{v} = \sum_i \theta_\mathbf{i} \mathbf{v_i} = \mathbf{V}\boldsymbol{\theta} \tag{2.38}$$

where $\boldsymbol{v}_i \triangleq \mathbf{A}_i \boldsymbol{v}$ and $\boldsymbol{V} \triangleq [\boldsymbol{v}_1 \ldots \boldsymbol{v}_{m+n-1}]$.

Because of the Toeplitz structure, it is straightforward to show that $\boldsymbol{V}$ is of full row rank if $\boldsymbol{v} \neq \mathbf{0}$ [37]. Then for any $\boldsymbol{\epsilon}$, $\boldsymbol{\theta} = \epsilon \boldsymbol{V}^\dagger \boldsymbol{k}$ satisfies $\mathbf{A}(\boldsymbol{\alpha} + \theta)\boldsymbol{v} = \boldsymbol{V}\epsilon\boldsymbol{V}^\dagger\boldsymbol{k} = \epsilon\boldsymbol{k}$ as desired. The same argument follows similarly for the Hankel structure or any other structure for which $\boldsymbol{V}$ is of full row rank.

Theorem 2.5.4. *For Toeplitz or Hankel structured problems, every point* $\boldsymbol{\alpha}$ *such that* $\mathbf{A}(\boldsymbol{\alpha})^T\mathbf{A}(\boldsymbol{\alpha})$ *is singular, lies on an n-dimensional hyperplane of consistent systems.*

Proof:

Let $\boldsymbol{v} \in$ *Null*$(\mathbf{A})$ *and* $\mathbf{V} = \mathbf{U}[\boldsymbol{\Sigma}\,\mathbf{0}][\mathbf{V_1}\,\mathbf{V_2}]^{\mathbf{T}}$ *be the Singular Value Decomposition [38] of* $\mathbf{V}$ *defined after (2.38). Then* $\mathbf{A}(\alpha+\boldsymbol{\epsilon})\boldsymbol{v} = \mathbf{V}\boldsymbol{\epsilon} = \beta_{\mathbf{0}}\mathbf{y}$ *has solution:*

$$\boldsymbol{\epsilon} = \beta_0\mathbf{V}^{\dagger}\mathbf{y} + \mathbf{V_2}\boldsymbol{\beta} \;=\; \beta_0\mathbf{V_1}\boldsymbol{\Sigma}^{-\mathbf{1}}\mathbf{U}\mathbf{y} + \mathbf{V_2}\boldsymbol{\beta} \tag{2.39}$$

$$\;=\; [\mathbf{V_1}\boldsymbol{\Sigma}^{-\mathbf{1}}\mathbf{U}\;\;\mathbf{V_2}]\tilde{\boldsymbol{\beta}} \tag{2.40}$$

for all $\tilde{\boldsymbol{\beta}} = [\beta_0\;\boldsymbol{\beta}]^T \in \mathbb{R}^n$. *Therefore, since* $\mathbf{V_1}$ *and* $\mathbf{V_2}$ *are orthogonal, any vector* $\mathbf{y}$ *is in Range*$(\mathbf{A}(\boldsymbol{\alpha}+\boldsymbol{\epsilon}))$ *for any* $\boldsymbol{\epsilon}$ *which is in the n-dimensional columnspace of* $[\mathbf{V_1}\boldsymbol{\Sigma}^{-\mathbf{1}}\mathbf{U}\;\;\mathbf{V_2}]$.

Theorems 2.5.3 and 2.5.4 illustrate the ill-conditioned nature of the consistency constraints. Note that the structure in (2.34) is Toeplitz and the singularity lies in a one dimensional plane of consistent systems. Theorems 2.5.2 and 2.5.4 show that, the rotation property and the proximity of consistencies to singularities are valid for many systems of interest with arbitrary dimensions. Therefore, the above observations for the simple example (2.34) are commonly encountered in practice.

2.6 Solution Techniques

2.6.1 Solving the SLS-BDU Optimization Problem

In this section, three iterative techniques are presented to solve the non-convex optimization problem of the SLS-BDU approach.

Individual Optimization by Alternating Minimizations

Although the SLS-BDU cost function is non-convex in $\mathbf{x}$ and $\boldsymbol{\alpha}$ together, it is convex for $\mathbf{x}$ and $\boldsymbol{\alpha}$ individually. It is easy to see that for a fixed $\boldsymbol{\alpha}$, the cost function is convex over $\mathbf{x}$. The following derivation shows that for a fixed $\mathbf{x}$, the cost is convex over $\boldsymbol{\alpha}$ as well.

$$\left\| (\mathbf{A}\mathbf{x} - \mathbf{y}) + \sum_i \alpha_i (\mathbf{A}_i \mathbf{x} - \mathbf{y}_i) \right\| = \| (\mathbf{A}\mathbf{x} - \mathbf{y}) + \boldsymbol{U}(\mathbf{x})\boldsymbol{\alpha} \| \quad ,$$

$$\text{where } \boldsymbol{U}(\mathbf{x}) \triangleq [(\mathbf{A}_1\mathbf{x} - \mathbf{y}_1) \; ... \; (\mathbf{A}_p\mathbf{x} - \mathbf{y}_p)] \quad .$$

which is convex over $\boldsymbol{\alpha}$ for a fixed $\mathbf{x}$. Therefore alternating minimizations as in the minimization of Extended Least Squares criterion [31], can be performed:

Algorithm 1. Alternating Minimizations

$\mathbf{x}^0 \leftarrow \mathbf{A}^\dagger \mathbf{y}$, $k \leftarrow 0$

while $\left\| \mathbf{x}^k - \mathbf{x}^{k-1} \right\| > \epsilon$ **do**

$\boldsymbol{\alpha}^{k+1} \leftarrow \arg\min_{\|\mathbf{W}\boldsymbol{\alpha}\| \leq \rho} \left\| (\mathbf{A}\mathbf{x}^k - \mathbf{y}) + \boldsymbol{U}(\mathbf{x}^k)\boldsymbol{\alpha} \right\|$

$\mathbf{x}^{k+1} \leftarrow \arg\min_{\mathbf{x}} \left\| \mathbf{A}(\boldsymbol{\alpha}^{k+1})\mathbf{x} - \mathbf{y}(\boldsymbol{\alpha}^{k+1}) \right\|$

$k \leftarrow k + 1$

end while

$\mathbf{x}_{Min-Min} \leftarrow \mathbf{x}^k$

Note that for the $\boldsymbol{\alpha}$ update in the alternating minimizations, a Quadratically Constrained Quadratic Program (QCQP) needs to be solved [39]. The advantage of this simple algorithm is that, the QCQP can be replaced with any other convex optimization and any choice of norm p, $1 \leq p \leq \infty$ can also be used. It is also possible to bound the perturbations by using multiple constraints of the form $\|\mathbf{W}_i\boldsymbol{\alpha}\| \leq \epsilon_i$, $i = 1, ..., P$, as well.

This alternating minimizations approach is widely used for optimizing a non-convex function over two sets of variables in applications such as super-resolution

and image deblurring [40]. By Proposition 2.7.1 of [41], Algorithm 1 is guaranteed to converge globally to a stationary point of the problem.

Joint Optimization by Linearization

The SLS-BDU cost function can also be linearized around a given $(\mathbf{x}, \boldsymbol{\alpha})$ for a small perturbation $[\boldsymbol{\Delta}\mathbf{x},\ \boldsymbol{\Delta}\boldsymbol{\alpha}]$ by ignoring second order terms as in [42]:

$$\begin{aligned} &\|(\mathbf{A}(\boldsymbol{\alpha}+\boldsymbol{\Delta}\boldsymbol{\alpha}))(\mathbf{x}+\boldsymbol{\Delta}\mathbf{x})-\mathbf{y}\| \approx \\ &\|\mathbf{A}(\boldsymbol{\alpha})\mathbf{x}-\mathbf{y}+\mathbf{U}(\mathbf{x})\boldsymbol{\Delta}\boldsymbol{\alpha}+\mathbf{A}(\boldsymbol{\alpha})\boldsymbol{\Delta}\mathbf{x}\|\,. \end{aligned} \tag{2.41}$$

Then, the solution to the following optimization provides an update on the estimated $\mathbf{x}$ and $\boldsymbol{\alpha}$:

$$\min_{\substack{\boldsymbol{\Delta}\mathbf{x},\boldsymbol{\Delta}\boldsymbol{\alpha} \\ \|\mathbf{W}(\boldsymbol{\alpha}+\boldsymbol{\Delta}\boldsymbol{\alpha})\|\leq\epsilon}} \left\| [\mathbf{A}(\boldsymbol{\alpha}) \quad \boldsymbol{U}(\mathbf{x})] \begin{bmatrix} \boldsymbol{\Delta}\mathbf{x} \\ \boldsymbol{\Delta}\boldsymbol{\alpha} \end{bmatrix} + (\mathbf{A}(\boldsymbol{\alpha})\mathbf{x}-\mathbf{y}) \right\|. \tag{2.42}$$

The following Newton iterations can be used to yield an estimate for the solution to the SLS-BDU problem in (2.12):

Algorithm 2. Newton's Method

$\mathbf{x}^0 \leftarrow \mathbf{A}^\dagger\mathbf{y}$, $\boldsymbol{\alpha}^0 \leftarrow 0$, $k \leftarrow 0$

while $\left\|\mathbf{x}^k - \mathbf{x}^{k-1}\right\| > \epsilon$ **do**

Solve (2.42) for $\Delta\mathbf{x}$ and $\Delta\boldsymbol{\alpha}$ by using QCQP

$\mathbf{x}^{k+1} \leftarrow \mathbf{x}^k + \Delta\mathbf{x}$

$\boldsymbol{\alpha}^{k+1} \leftarrow \boldsymbol{\alpha}^k + \Delta\boldsymbol{\alpha}$

$k \leftarrow k+1$

end while

$\mathbf{x}_{Min-Min} \leftarrow \mathbf{x}^k$

This algorithm is a hybrid of Gauss Newton method and Sequential Quadratic Programming (SQP). Assuming $\mathbf{A}(\boldsymbol{\alpha})$ is nonsingular for $\|\mathbf{W}\boldsymbol{\alpha}\| \leq \rho$, it converges locally quadratically to a stationary point by Theorem 12.4.1 [43].

Fixed point iteration using the Fréchet derivatives

By using Theorem 2.5.1, the gradient of the Lagrangian of problem (2.20) can be written as:

$$\frac{1}{2}\nabla\mathcal{L}(\boldsymbol{\alpha},\lambda) = \mathbf{y}(\boldsymbol{\alpha})^{\mathbf{T}}\mathbf{P}_{\boldsymbol{\alpha}}^{\perp}(\mathbf{y}_i - \mathbf{A}_i\mathbf{A}(\boldsymbol{\alpha})^{\dagger}\mathbf{y}(\boldsymbol{\alpha})) + \lambda\boldsymbol{\alpha}. \tag{2.43}$$

By solving λ under the constraint of $\|\mathbf{W}\boldsymbol{\alpha}\|_2 = \rho$, we obtain:

$$\rho\mathbf{f}(\boldsymbol{\alpha}) = \boldsymbol{\alpha}\,\|\mathbf{W}\mathbf{f}(\boldsymbol{\alpha})\|_{\mathbf{2}} \quad , \tag{2.44}$$

where $\mathbf{f}_i(\boldsymbol{\alpha}) \triangleq \mathbf{y}(\boldsymbol{\alpha})^{\mathbf{T}}\mathbf{P}_{\boldsymbol{\alpha}}^{\perp}(\mathbf{A}_i\mathbf{A}(\boldsymbol{\alpha})^{\dagger}\mathbf{y}(\boldsymbol{\alpha}) - \mathbf{y}_i)$, $i = 1, ..., p$. As given below, a fixed point iteration to solve (2.44) can be used to find the SLS-BDU estimate. Note that although this fixed point iteration converges faster, it can only be used for the Euclidean norm.

Algorithm 3. Fixed Point Iteration

$\boldsymbol{\alpha}^0 \leftarrow 0$, $k \leftarrow 0$

while $\left\|\boldsymbol{\alpha}^k - \boldsymbol{\alpha}^{k-1}\right\| > \epsilon$ **do**

$\boldsymbol{\alpha}^{k+1} \leftarrow \frac{\rho\mathbf{f}(\boldsymbol{\alpha}^{\mathbf{k}})}{\left\|\mathbf{W}\mathbf{f}(\boldsymbol{\alpha}^{\mathbf{k}})\right\|_2}$

$k \leftarrow k + 1$

end while

$\boldsymbol{\alpha}^* \leftarrow \boldsymbol{\alpha}^k$, $\mathbf{x}_{Min-Min} \leftarrow \mathbf{A}(\alpha^*)^{\dagger}\mathbf{y}(\alpha^*)$

In our numerical experiments, we observed that this fixed point iteration has superior convergence. In the appendix we give a proof for the local Lipschitz continuity of $\nabla_{\boldsymbol{\alpha}}\left\|\mathbf{P}_{\boldsymbol{\alpha}}^{\perp}\mathbf{y}(\boldsymbol{\alpha})\right\|_2^2$ provided that there exists no singularity or consistency inside the constraint set $\|\mathbf{W}\boldsymbol{\alpha}\| \leq \rho$. Then by Proposition A.26 of [41],

Algorithm 3 convergences to a stationary point with geometric rate of convergence.

Remark 4. *The convergence criterion of Algorithm 3 makes the need of such a norm constraint clearer. Note that the Lipschitz continuity would fail near a singularity.*

2.6.2 Choosing The Bound Parameter Based on the Gradient Norm

The SLS-BDU technique requires a bound on $\boldsymbol{\alpha}$. Such a bound may be readily available when uncertainty bounds on the matrix elements are known. However, for those cases when there exists no such descriptive information on the bound on $\boldsymbol{\alpha}$, it is desirable to have a robust scheme to determine the bound which yields a good tradeoff between $\|\mathbf{A}(\alpha^*) - \mathbf{A}_0\|$ and $\left\|\mathbf{A}^\dagger(\boldsymbol{\alpha})\right\|_F$. In this section we provide such a criterion based on the gradient norm. Inspecting the example of Section IV in Figure 2.1, it can be concluded that an abrupt increase in the gradient norm of the lower bound results in estimates which are highly sensitive to $\boldsymbol{\alpha}$, loosing robustness. Hence, we investigated the following simple strategy in the choice of the bound ρ. As given in Algorithm 4, we start with $\rho = 0$ and increase it with small steps $\Delta\rho$ till the gradient norm $\|\mathbf{f}(\boldsymbol{\alpha})\|_2$ starts to increase. In a wide range of experiments we observed that this simple scheme provides highly effective results. In the next section, we illustrate its performance over a range of simulations conducted at different noise levels.

Algorithm 4. Automated Selection of Bound Parameter

$\rho^0 \leftarrow 0$, $k \leftarrow 0$, $\mathbf{f}(\boldsymbol{\alpha})^0 \leftarrow 0$, $\mathbf{f}(\boldsymbol{\alpha})^{-1} \leftarrow 1$
while $\left\|\mathbf{f}(\boldsymbol{\alpha})^k\right\|_2 < \left\|\mathbf{f}(\boldsymbol{\alpha})^{k-1}\right\|_2$ **do**
  $(\mathbf{x}^k, \mathbf{f}(\boldsymbol{\alpha})^k) \leftarrow$ **Algorithm 3**$(\rho^k, \mathbf{A}, \mathbf{y})$

$\rho \leftarrow \rho + \Delta\rho$

$k \leftarrow k + 1$

end while

$\hat{\mathbf{x}} \leftarrow \mathbf{x}^k$

2.7 Applications and Numerical Results

Verification of Theorem 2.3.2

First we verify the accuracy of our result in (2.25). A Toeplitz matrix $\mathbf{A}_0$ with smallest singular value σ_0 is generated and perturbed with an unknown $\boldsymbol{\theta}$ to obtain the measured matrix $\mathbf{A}$ as in (2.11). Based on the observation $\mathbf{y} = \mathbf{A}_0\mathbf{x}_0 + \mathbf{w}$ and $\mathbf{A}$ only, $\mathbf{x}_0$ is estimated using SLS-BDU and STLS for a range of σ_0 and SNR= $\frac{\|x\|_2^2}{n\sigma_w^2}$ values while θ is fixed and $\|\theta\|_2 = 0.5$. The theorem specifies a region in (SNR, σ_0) plane where the MSE of SLS-BDU is smaller than STLS asymptotically as shown in Figure 2.4(a). For comparison, the empirical probability of $\|\mathbf{x}_{SLS-BDU} - \mathbf{x}_0\| < \|\mathbf{x}_{STLS} - \mathbf{x}_0\|$ in 100 trials is shown in Figure 2.4(b). Although the theoretical region is conservative, it clearly indicates the ill conditioned small σ_0 and low SNR region where SLS-BDU outperforms with probability approaching one.

Next we discuss three signal processing applications of the SLS-BDU approach to illustrate its effectiveness in ill conditioned problems.

ϵ_b/b_{true}	0.2	0.6
$\|\mathbf{x}_{true} - \mathbf{x}_{LS}\| \,/\, \|\mathbf{x}_{true}\|$	0.0820	0.2123
$\|\mathbf{x}_{true} - \mathbf{x}_{SLS-BDU}\| \,/\, \|\mathbf{x}_{true}\|$	0.0274	0.1279
$\|\mathbf{H}_{true} - \mathbf{H}_{SLS-BDU}\|_{\mathrm{F}} \,/\, \|\mathbf{H}_{true}\|_{\mathrm{F}}$	0.1072	0.2589
$\|\mathbf{H}_{true} - \mathbf{H}_{SLS-BDU}\|_{\mathrm{F}} \,/\, \|\mathbf{H}_{true}\|_{\mathrm{F}}$	0.0655	0.1284

Table 2.1: $\mathbf{x}_{true}$, $\mathbf{x}_{LS}$ and $\mathbf{x}_{SLS-BDU}$ correspond to actual signal and estimates, $\mathbf{H}_{true}$, $\mathbf{H}$, $\mathbf{H}_{SLS-BDU}$ correspond to actual, nominal and corrected matrices respectively.

Deconvolution under Impulse Response Uncertainties

Suppose that the observed signal is the output of an LTI system with impulse response $h[n]$:

$$y[n] = \sum_{k=0}^{L-1} x[n-k]h[k] + w[n], \tag{2.45}$$

where and $w[n]$ is white Gaussian noise and:

$$h[n] = \sum_{i=1}^{p} (a_i + \delta a_i) e^{-(b_i+\delta b_i)n} \cos(w_i n + \phi_i) \quad , \tag{2.46}$$

with bounded data uncertainties on coefficients $\mid \delta a_i \mid < \epsilon_{a_i}$ and damping terms $\mid \delta b_i \mid < \epsilon_{b_i}$, $i = 1, ..., p$. We want to recover $x[n]$ under this structured uncertainty on the impulse response $h[n]$. The uncertainties in b_i's can be linearized by a first order approximation, $e^{-(b_i+\delta b_i)n} \approx e^{-b_i n}(1 - \delta b_i n)$, to obtain the following

$$\mathbf{y} = (\mathbf{H} + \sum_{i=1}^{p} \alpha_i \mathbf{H}_i)\mathbf{x} + \mathbf{w} \,,$$

with the constraint $\|\mathbf{W}\boldsymbol{\alpha}\|_{\infty} \leq \epsilon$. Here $\mathbf{H}$ and $\mathbf{H}_i$ are Toeplitz structured matrices which perform convolution operation with the terms in the summation of (2.46) and α_i's stand for the unknown perturbations $\delta a_i, \delta b_i$.

The impulse response $h[n]$ with uncertainties is shown in Fig. 2.5(a). As shown in Figure 2.5(b), the SLS-BDU estimate closely approximates the actual input signal. Table 2.1 provides comparison results between the SLS-BDU and least squares estimates for both the input signal and the impulse response estimates at two different uncertainty levels. As expected based on Theorem 3.2,

SNR	4dB	7dB	10dB
LS	0.0347	0.0344	0.0346
TLS	0.0308	0.0295	0.0298
STLS	0.0297	0.0304	0.0321
HTLS	0.0311	0.0309	0.0275
SLS-BDU	0.0279	0.0249	0.0241

Table 2.2: Average Frequency Estimation Errors for LS, TLS, STLS, HTLS and SLS-BDU

the tabulated results show that the SLS-BDU technique provides significantly better estimates for both the input and the impulse response. Note that STLS estimate is unsatisfactory since the perturbations are not bounded and linear approximation is not valid for large perturbations.

Frequency Estimation of Multiple Sinusoids

Consider the case where parameters of two complex sinusoids which are close in frequency need to be estimated with frequencies $f_1 = 0.12$ Hz and $f_2 = 0.10$ Hz in white noise w_n:

$$x(n) = \exp(2\pi j f_1 n) + \exp(2\pi j f_2 n) + w_n,\ n = 0, 1, \ldots, 25. \tag{2.47}$$

The following Linear prediction equations can be solved to estimate the parameters of L sinusoids [24]:

$$\begin{bmatrix} x_1 & x_2 & \cdots & x_L \\ x_2 & x_3 & \cdots & x_{L+1} \\ x_3 & \iddots & & \vdots \\ \vdots & & \iddots & x_{N-2} \\ x_{N-L} & \cdots & \cdots & x_{N-1} \end{bmatrix} \mathbf{z} = \begin{bmatrix} x_{L+1} \\ x_{L+2} \\ x_{L+3} \\ \vdots \\ x_N \end{bmatrix}. \tag{2.48}$$

The frequency estimation error defined by $\sqrt{(\hat{f}_1 - f_1)^2 + (\hat{f}_2 - f_2)^2}$ is evaluated for the estimates with SLS-BDU with parameters $\rho = 1.3$ and $\mathbf{W} = \mathbf{I}$ in

1000 independent trials at various SNR values. In table 2.2, a comparison of LS, TLS, STLS, HTLS [44] and SLS-BDU is given. Histograms of estimation errors are plotted in Figure 2.6. As expected based on Theorem 3.2, the tabulated results and histograms reveal that the SLS-BDU estimator not only provides more accurate estimates on the average but it is also significantly more robust than the STLS estimator. As indicated by the obtained histograms, the errors of SLS-BDU estimates have higher concentration around zero, whereas STLS and HTLS estimates have heavy tailed distributions.

System Identification

Consider the system identification setup depicted in Figure 2.7. An input sequence u_0 is applied to the FIR filter $H(z)$ and the output y_0 is generated. Measurements of the input and the output contain noise w_i and w_o respectively. The identification of the filter $H(z)$ can be cast as the following regression problem [16]:

$$\mathbf{U_0 h = y_0} \tag{2.49}$$

Where $\mathbf{U = U_0 + W_i}$ is the observed noisy Toeplitz matrix and $\mathbf{y = y_0 + w_o}$ is the observed noisy output. The filter coefficients were set to $\mathbf{h} = [-0.3, -0.9, 0.8]^T$, the training signal $\mathbf{u_0}$ was selected as a random sequence of ± 1's and equal variance independent white noise was added to input and output. SLS-BDU estimates are generated with autonomously chosen bound ρ by using Algorithm 4. The MSE in 10000 independent trials of the SLS-BDU estimator, and RSTLS for a range of regularization parameters are shown in Figure 2.8. As seen from these results, the SLS-BDU estimator with autonomously chosen bound ρ provides lower MSE than the RSTLS estimates that are obtained with a range of regularization parameters. In this example, to illustrate the effectiveness of the criterion by which Algorithm 4 determines ρ, we included the performance of

SLS-BDU estimates with hand tuned ρ as well. As seen from the obtained results, the autonomous choice provides performance results that are close to the hand tuned case.

The implementations of STLS and RSTLS used in numerical comparisons are [45, 46] respectively and both available online. And for TLS and HTLS methods direct implementations of corresponding references are used.

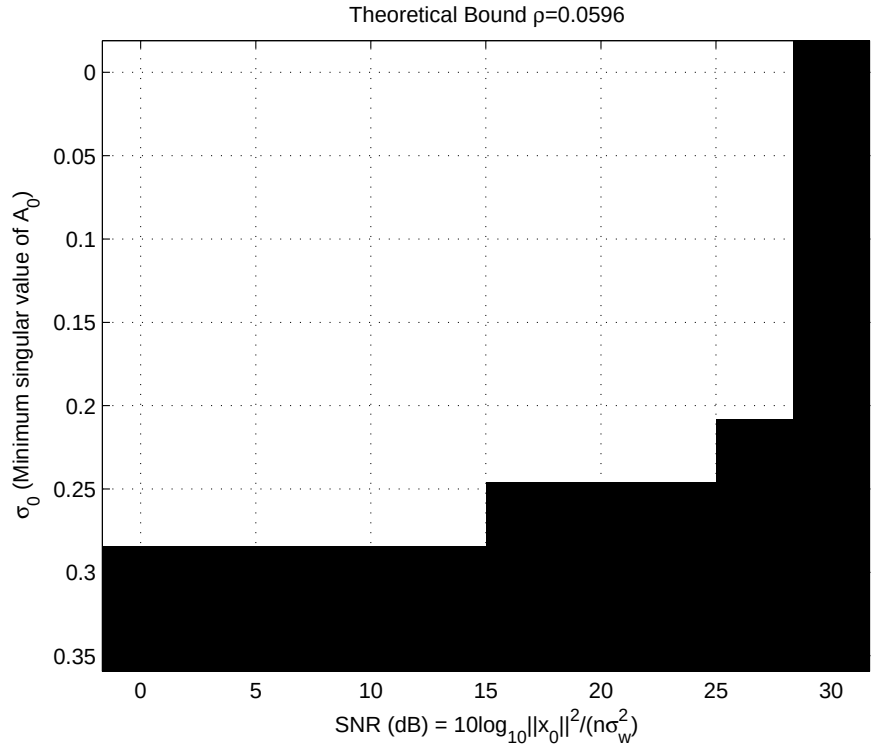

(a) Theoretical Bound

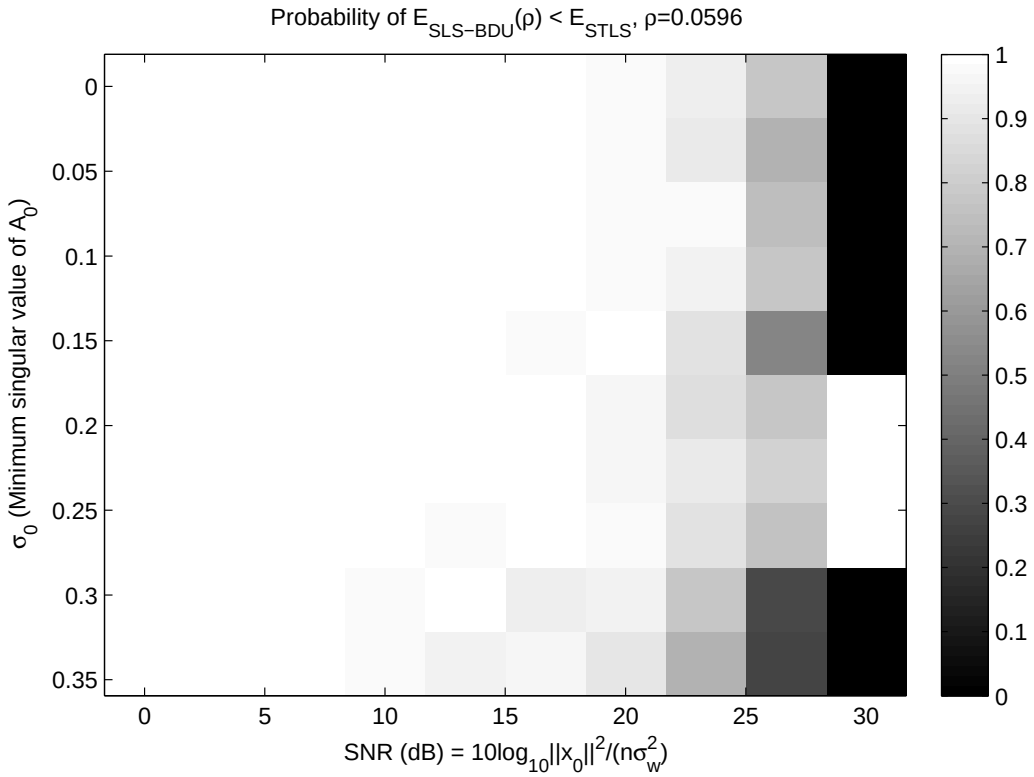

(b) Empirical Probability

Figure 2.4: Comparison of SLS-BDU and STLS

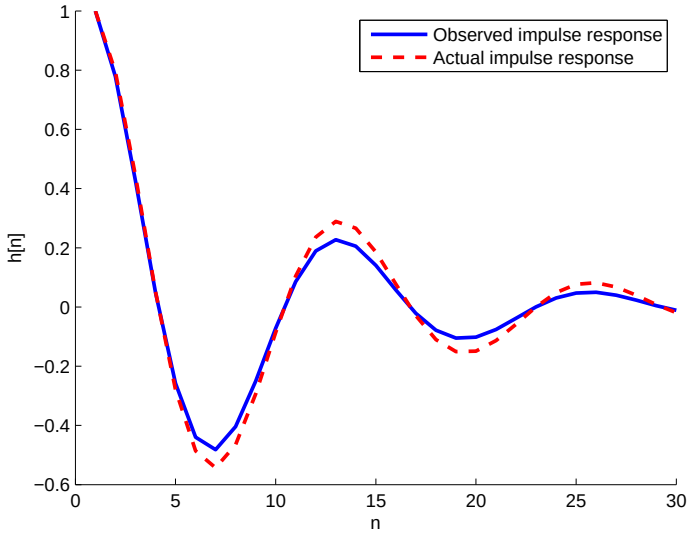

(a) True (dashed) and observed (solid) impulse responses

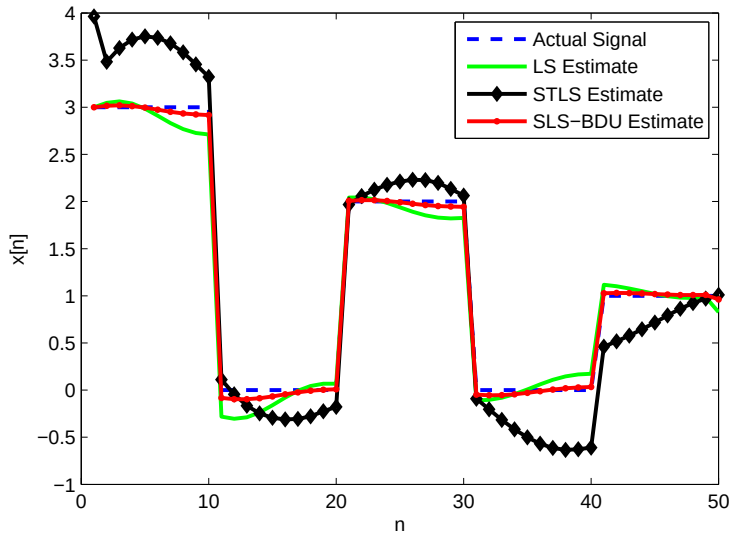

(b) Actual and restored input signals $\mathbf{x}$ are shown in dashed and solid lines respectively

Figure 2.5: Deconvolution under Impulse Response Uncertainties

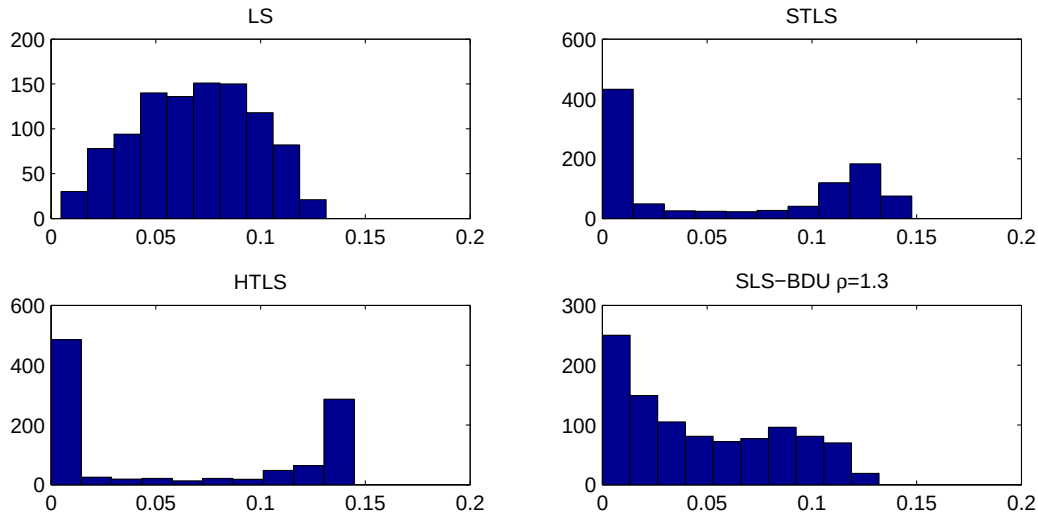

Figure 2.6: Histogram of frequency estimation errors for LS, STLS, HTLS and SLS-BDU. Note that the distribution of the estimation error is heavy tailed for STLS and HTLS.

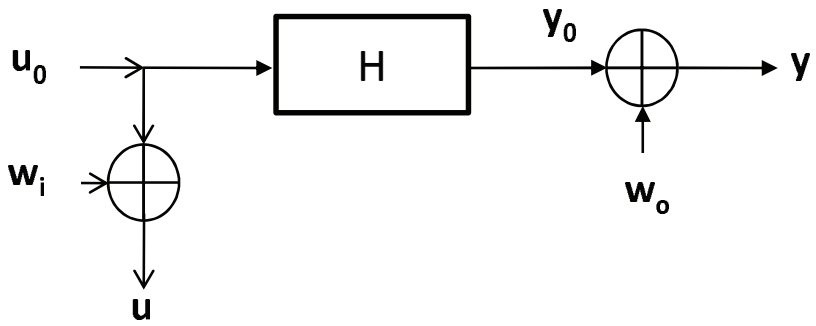

Figure 2.7: System identification with noisy input u and noisy output y.

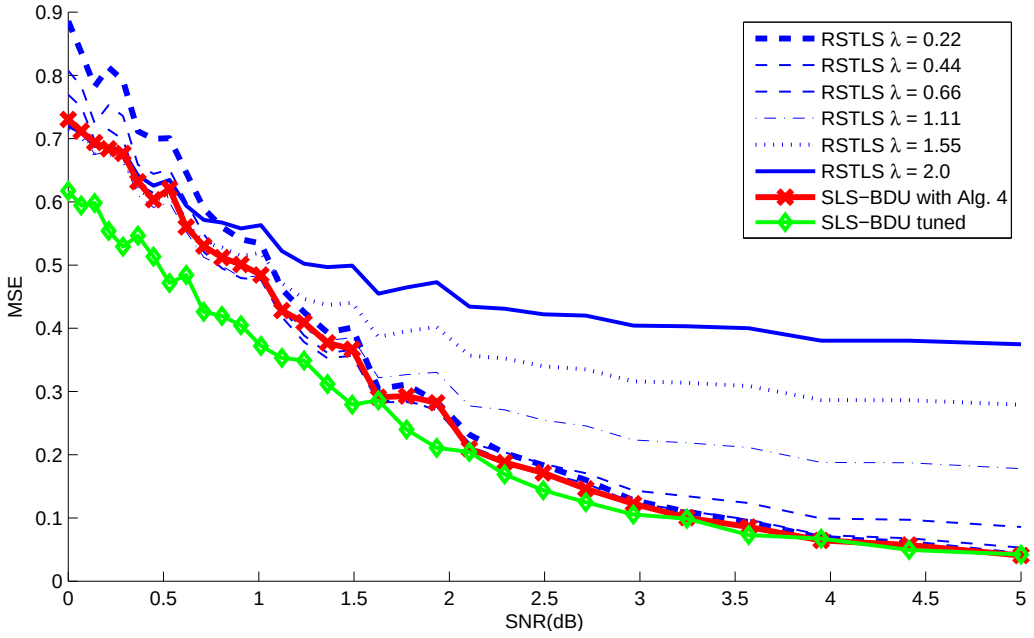

Figure 2.8: MSE of Algorithm 4 and RSTLS solutions for a range of regularization parameters vs SNR.

Chapter 3

SPARSE UNCERTAINTY

3.1 Sparse Signal Processing

It is well known that, the Least Squares (LS) method for solving the overdetermined linear equations $\mathbf{A}_0\mathbf{x} = \mathbf{y}$ for $m > n$, is the Maximum Likelihood solution when the observations $\mathbf{y} = \mathbf{y}_0 + \mathbf{e}$ are subject to independent identically distributed Gaussian noise vector $\mathbf{e}$ and recovers $\mathbf{x}_0$ with some error [2]. Surprisingly, it was recently shown that, if $\mathbf{e}$ is sparse, exact recovery of $\mathbf{x}_0$ can be achieved for some classes of matrices $\mathbf{A}$ using linear programming [47]. However, in practice the elements of the coefficient matrix are also subject to errors since they may be results of some other measurements or obtained under some modeling assumptions. When there are errors in both, i.e., $\mathbf{A} = \mathbf{A}_0 + \mathbf{E}$ and $\mathbf{y} = \mathbf{y}_0 + \mathbf{e}$, the Total Least Squares (TLS) technique, which "corrects" the system with minimum perturbation so that it becomes consistent is widely used [3]. TLS also have Maximum Likelihood properties when the perturbations are zero mean i.i.d. Gaussian random variables.

It is known that the Total Least Squares problem is more ill-conditioned than the Least Squares problem because the amount of uncertainty greatly increases

when we introduce perturbations in $\mathbf{A}$ [3]. Inspired by [47], we seek a TLS complement of that result and show in the next section that, if the perturbations $\mathbf{E}$ and $\mathbf{e}$ are sparse in some basis, then we may recover both the perturbations and the unknown $\mathbf{x}$ by knowing only the perturbed data $(\mathbf{A}_0 + \mathbf{E}, \mathbf{y}_0 + \mathbf{e})$.

3.2 Novel Sparse Perturbation Theory

Assume a true, consistent, overdetermined linear system of equations, $\mathbf{A}_0\mathbf{x}_0 = \mathbf{y}_0$, while the observed quantities are related via:

$$\mathbf{A} = \mathbf{A}_0 + \sum_{i=1}^{N} \mathbf{A}_i p_i \ , \qquad \mathbf{y} = \mathbf{y}_0 + \sum_{i=1}^{N} \mathbf{y}_i p_i \ \ , \tag{3.1}$$

where matrices $\mathbf{A}_i$ and vectors $\mathbf{y}_i$ are constants which form a possibly overcomplete basis for the perturbation $\mathbf{p} = [p_1 \dots p_N]^T$.

Case I: $\mathbf{x}_0$ is known Although the case where $\mathbf{x}_0$ is known might seem fictitious, there exists applications such as channel identification, which we design the signal $\mathbf{x}_0$ to sense the system matrix $\mathbf{A}$. This recovery scheme is known as Matrix Identification [48] and recently applied for Compressed Sensing Radar [49]. First we define the Restricted Isometry Constant (RIC) of a matrix. Then the following theorem demonstrates exact recovery of the perturbation using Basis Pursuit (BP).

Definition 3. *For $s \in \mathbb{Z}^+$, define restricted isometry constant (RIC) δ_s of a matrix $\mathbf{\Phi}$ as the smallest nonnegative number such that*

$$(1 - \delta_s) \left\|\mathbf{x}\right\|_2^2 \leq \left\|\mathbf{\Phi}\mathbf{x}\right\|_2^2 \leq (1 + \delta_s) \left\|\mathbf{x}\right\|_2^2 \tag{3.2}$$

holds for all vectors $\mathbf{x}$ which are s-sparse, i.e., have atmost s nonzero elements [50].

Theorem 3.2.1. *(Exact Recovery) Let $\mathbf{p}$ be a k-sparse vector and δ_s be the RIC for,*

$$\mathbf{\Phi}(\mathbf{x}_0) \triangleq \Big[\mathbf{A}_1\mathbf{x}_0 - \mathbf{y}_1\Big| \ \cdots \ \Big|\mathbf{A}_N\mathbf{x}_0 - \mathbf{y}_N\Big]. \tag{3.3}$$

and $\delta_{2k} < \sqrt{2} - 1$. *Then the following convex program:*

$$\min \|\mathbf{p}'\|_1 \quad s.t. \quad (\mathbf{A} - \sum_{i=1}^{N} \mathbf{A}_i p_i')\mathbf{x}_0 = \mathbf{y} - \sum_{i=1}^{N} \mathbf{y}_i p_i' \tag{3.4}$$

recovers $\mathbf{A}_0$ *exactly.*

Proof:

Using (3.1) we get:

$$(\mathbf{A} - \sum_{i=1}^{N} \mathbf{A}_i p_i)\mathbf{x}_0 = \mathbf{y} - \sum_{i=1}^{N} \mathbf{y}_i p_i \quad , \tag{3.5}$$

$$\mathbf{A}\mathbf{x}_0 - \mathbf{y} = \sum_{i=1}^{N} (\mathbf{A}_i \mathbf{x}_0 - \mathbf{y}_i) p_i \quad , \tag{3.6}$$

$$\mathbf{A}\mathbf{x}_0 - \mathbf{y} = \mathbf{\Phi}(\mathbf{x}_0)\mathbf{p} \quad , \tag{3.7}$$

When $\mathbf{x}_0$ is known, $\mathbf{\Phi}(\mathbf{x}_0) \in \mathbb{R}^{m \times N}$ is a known overcomplete dictionary satisfying Retricted Isometry Property (RIP) and the convex program (3.4) recovers the perturbation $\mathbf{p}$ as shown in [50] and therefore $\mathbf{A}_0$ is recovered exactly. If $N \leq m$ then recovery is trivial via directly solving (3.7) if $\mathbf{\Phi}(\mathbf{x}_0)$ is full rank.

Remark 5. *It is straightforward to show that Toeplitz structured perturbations* $\mathbf{A}_i$ *with* $\mathbf{y}_i = 0, \forall i$ *result a Toeplitz* $\mathbf{\Phi}(\mathbf{x}_0)$. *It is known that deterministic Toeplitz matrices satisfy RIP of order* $\mathcal{O}(n^\gamma)$ *if* $\mathbf{x}_0$ *is deterministic and satisfies the PDACF property with* γ *[51]. If* $\mathbf{x}_0$ *is random, it is shown that Toeplitz matrices satisfy RIP of order k for many practical distributions, with probability exceeding* $1 - \exp(c_1 \frac{n}{k^2})$ *if* $k \leq c_2 \sqrt{\frac{n}{N}}$ *where* c_1, c_2 *are constants [52].*

Instead of RIP we can derive a sufficiency condition as follows:

Theorem 3.2.2. *(Coherency of perturbations) Assume* $\mathbf{A}_i \mathbf{x}_0 \neq \mathbf{y}_i \quad \forall i$. *If* $\mu < \frac{1}{2k-1}$ *, where,*

$$\mu \triangleq \max_{i \neq j} \frac{< \mathbf{A}_i \mathbf{x}_0 - \mathbf{y}_i, \mathbf{A}_j \mathbf{x}_0 - \mathbf{y}_j >}{\|\mathbf{A}_i \mathbf{x}_0 - \mathbf{y}_i\|_2 \|\mathbf{A}_j \mathbf{x}_0 - \mathbf{y}_j\|_2}, \tag{3.8}$$

then the convex program (3.4) recovers the perturbation exactly.

Corollary 3.2.3. *If perturbations are unstructured as in the Total Least Squares problem then* $\mathbf{A}_i$ *are the standart basis and it is trivial to show that* $\mu = 1$ *and sparse perturbations can not be recovered exactly via any method. On the contrary, if perturbations are orthogonal, i.e.,* $\mathbf{A}_i^T\mathbf{A}_j = \mathbf{y}_i^T\mathbf{y}_j = \mathbf{A}_i^T\mathbf{y}_j = 0, \ \ \forall i \neq j$ *then* $\mu = 0$.

Case II: $\mathbf{x}_0$ is not known This is the general case examined in this section and differs significantly from the usual setup of sparse recovery since the dictionary $\mathbf{\Phi}(\mathbf{x}_0)$ is unknown. A straightforward workaround is to employ the Least Squares solution $\mathbf{A}^\dagger\mathbf{y}$ of $\mathbf{x}_0$ and apply a regularized Basis Pursuit [53] with the estimate $\mathbf{\Phi}(\mathbf{A}^\dagger\mathbf{y})$. Using the recent results of [54] on dictionary perturbations we next prove that this scheme provides stable recovery under some conditions.

Theorem 3.2.4. *(Stable Recovery) For a k-sparse* $\mathbf{p}$*, if RIC of* $\mathbf{\Phi}(\mathbf{x}_0)$ *satisfies:*

$$\delta_{2k} < \frac{\sqrt{2}}{(1+2k\nu)^2} - 1 \quad , \textit{where} \quad \nu \triangleq \frac{\max\limits_i \quad \left\|\mathbf{A}_i(\mathbf{A}^\dagger\mathbf{y} - \mathbf{x}_0)\right\|_2}{\min\limits_j \quad \left\|\mathbf{A}_j\mathbf{x}_0 - \mathbf{y}_j\right\|_2} \quad , \tag{3.9}$$

and $k \leq m$*, then the following convex program:*

$$\min \left\|\mathbf{p}'\right\|_1 s.t. \left\|(\mathbf{A} - \sum_{i=1}^{N}\mathbf{A}_i p_i')\mathbf{A}^\dagger\mathbf{y} - (\mathbf{y} - \sum_{i=1}^{N}\mathbf{y}_i p_i')\right\|_2 \leq \boldsymbol{\epsilon} \tag{3.10}$$

provides stable recovery in the following sense:

$$\left\|\mathbf{p}^* - \mathbf{p}_0\right\|_2 \leq C\boldsymbol{\epsilon}, \tag{3.11}$$

where, $\mathbf{p}^*$ is the optimal solution of (3.10), C is a small constant and

$$\boldsymbol{\epsilon} \triangleq \left(k\nu\frac{\sqrt{1+\delta_k}}{\sqrt{1-\delta_k}} + \frac{\left\|\mathbf{A}(\mathbf{A}^\dagger\mathbf{y} - \mathbf{x}_0)\mathbf{y}\right\|_2}{\left\|\mathbf{r}\right\|_2}\right)\left\|\mathbf{r}\right\|_2 \quad , \tag{3.12}$$

i.e., the error is in the order of the norm of $\mathbf{r} \triangleq \mathbf{A}\mathbf{x}_0 - \mathbf{y}$ which is the residual of the perturbed system.

Proof:

Following the results of [54], we seek a bound for the worst case dictionary

perturbation over k columns when we use the Least Squares estimate $\mathbf{x} = \mathbf{A}^{\dagger}\mathbf{y}$ in (3.7):

$$\begin{aligned}
&\frac{\max\limits_{i_1,\ldots,i_k,i_p\neq i_q} \left\|[\mathbf{A}_{i_1}(\mathbf{x}-\mathbf{x}_0),\ldots,\mathbf{A}_{i_k}(\mathbf{x}-\mathbf{x}_0)]\right\|_2}{\max\limits_{i_1,\ldots,i_k,i_p\neq i_q} \left\|[(\mathbf{A}_{i_1}\mathbf{x}_0-\mathbf{y}_{i_1}),\ldots,(\mathbf{A}_{i_k}\mathbf{x}_0-\mathbf{y}_{i_k})]\right\|_2} \\
\leq\ & \frac{\max\limits_{i_1,\ldots,i_k,i_p\neq i_q} \sqrt{k} \max\limits_{i\in\{i_1,\ldots,i_k\}} \left\|\mathbf{A}_i(\mathbf{x}-\mathbf{x}_0)\right\|_2}{\max\limits_{i_1,\ldots,i_k,i_p\neq i_q} \left\|[(\mathbf{A}_{i_1}\mathbf{x}_0-\mathbf{y}_{i_1}),\ldots,(\mathbf{A}_{i_k}\mathbf{x}_0-\mathbf{y}_{i_k})]\right\|_2} \\
\leq\ & \frac{\max\limits_{i_1,\ldots,i_k,i_p\neq i_q} \sqrt{kR} \max\limits_{i\in\{i_1,\ldots,i_k\}} \left\|\mathbf{A}_i(\mathbf{x}-\mathbf{x}_0)\right\|_2}{\max\limits_{i_1,\ldots,i_k,i_p\neq i_q} \sum\limits_{j\in\{i_1,\ldots,i_k\}} \left\|\mathbf{A}_j\mathbf{x}_0-\mathbf{y}_j\right\|_2} \\
\leq\ & k\ \frac{\max\limits_{i} \left\|\mathbf{A}_i(\mathbf{x}-\mathbf{x}_0)\right\|_2}{\min\limits_{j} \left\|\mathbf{A}_j\mathbf{x}_0-\mathbf{y}_j\right\|_2},
\end{aligned} \tag{3.13}$$

$$\text{where } R = \mathit{Rank}[(\mathbf{A}_{i_1}\mathbf{x}_0-\mathbf{y}_{i_1}),\ldots,(\mathbf{A}_{i_k}\mathbf{x}_0-\mathbf{y}_{i_k})] \leq k.$$

The perturbation in the left side is also bounded by, $\frac{\|\mathbf{A}(\mathbf{x}-\mathbf{x}_0)\|_2}{\|\mathbf{A}\mathbf{x}_0-\mathbf{y}\|}$. A straightforward application of Theorem 2 of [54] using the derived perturbation bounds completes the proof.

Remark 6. *Note that the stability condition depends heavily on ν and consequently $\left\|\mathbf{A}^{\dagger}\mathbf{y}-\mathbf{x}_0\right\|$, which is known to scale with $\|\mathbf{A}\|_2^2 / \left\|\mathbf{A}^{\dagger}\right\|_2^2$, the square of the condition number of $\mathbf{A}$ [55]. In particular, since δ_{2k} is nonnegative, the theorem requires $\nu < \frac{\sqrt[4]{2}-1}{2k}$ for stable recovery. Therefore, we conclude that two major limitations of perturbation recovery is the ill-conditioning of $\mathbf{A}$ and coherency of perturbations.*

Remark 7. *By using a corrective Min-Min approach that will be introduced next, the performance of this estimator may be improved significantly.*

3.3 Proposed Estimator when $\mathbf{x}_0$ is not known

The following double minimization is proposed for joint estimation of the sparse perturbation $\mathbf{p}$ and unknown $\mathbf{x}_0$:

$$P_0 : \min_{\mathbf{x}} \min_{\|\mathbf{p}\|_0=k} \left\| (\mathbf{A} - \sum_{i=1}^{N} \mathbf{A}_i p_i)\mathbf{x} - (\mathbf{y} - \sum_{i=1}^{N} \mathbf{y}_i p_i) \right\|_2$$

3.3.1 Alternating Minimizations Algorithm to solve P_0

When $\mathbf{p}$ is fixed the problem reduces to a simple Least Squares problem which can be solved via the pseudoinverse. If $\mathbf{x}$ is fixed then there exists many algorithms to solve for a sparse $\mathbf{p}$ [56]. Therefore a local optimum can be found using an alternating minimizations algorithm [25] where we chose Orthogonal Matching Pursuit (OMP) [57] in the intermediate step for its simplicity:

Algorithm 1. Alternating Minimizations for P_0

$\mathbf{x}^0 \leftarrow \mathbf{A}^\dagger \mathbf{y}$, $\mathbf{p}^0 \leftarrow \mathbf{0}$, $k \leftarrow 0$

while $\left\|\mathbf{x}^k - \mathbf{x}^{k-1}\right\| > \Delta$ **do**

  $\mathbf{p}^{k+1} \leftarrow \arg\min_{\|\mathbf{p}\|_0=k} \left\|\mathbf{A}\mathbf{x}^k - \mathbf{y} - \mathbf{\Phi}(\mathbf{x}^k)\mathbf{p}^k\right\|$

  (using OMP)

  $\mathbf{x}^{k+1} \leftarrow (\mathbf{A} - \sum_{i=1}^{N} \mathbf{A}_i p_i)^\dagger (\mathbf{y} - \sum_{i=1}^{N} \mathbf{y}_i p_i)$

  $k \leftarrow k + 1$

end while

$\hat{\mathbf{A}} \leftarrow (\mathbf{A} - \sum_{i=1}^{N} \mathbf{A}_i p_i^k)$, $\hat{\mathbf{y}} \leftarrow (\mathbf{A} - \sum_{i=1}^{N} \mathbf{y}_i p_i^k)$, $\hat{\mathbf{x}} \leftarrow \mathbf{x}^k$

3.3.2 Convex Relaxation of the Proposed Estimator

If the constraint on $\mathbf{p}$ is relaxed to l_1 norm as follows, faster gradient based techniques can be used to solve the problem since the objective of P_0 is convex in both $\mathbf{x}$ and $\mathbf{p}$ (but not jointly):

$$P_1 : \min_{\mathbf{x}} \min_{\|\mathbf{p}\|_1 \leq t} \left\| (\mathbf{A} - \sum_{i=1}^{N} \mathbf{A}_i p_i)\mathbf{x} - (\mathbf{y} - \sum_{i=1}^{N} \mathbf{y}_i p_i) \right\|_2 .$$

First define the following matrix functions:

Definition 4. *Let,*

$$\mathbf{A}(\mathbf{p}) \triangleq \mathbf{A} - \sum_{i=1}^{N} \mathbf{A}_i p_i \quad , \qquad \mathbf{y}(\mathbf{p}) \triangleq \mathbf{y} - \sum_{i=1}^{N} \mathbf{y}_i p_i \quad . \tag{3.14}$$

Assuming $\mathbf{A}(\mathbf{p})$ is of full column rank for $\|\mathbf{p}\|_1 \leq t$, the outer minimization of P_1 can be carried out analytically as:

$$\min_{\|\mathbf{p}\|_1 \leq t} \min_{\mathbf{x}} \ \|\mathbf{A}(\boldsymbol{\alpha})\mathbf{x} - \mathbf{y}(\boldsymbol{\alpha})\|_2 = \min_{\|\mathbf{p}\|_1 \leq t} \left\|\mathbf{P}_{\mathbf{p}}^{\perp}\mathbf{y}(\mathbf{p})\right\|_2 \tag{3.15}$$

where $\mathbf{P}_{\mathbf{p}}^{\perp} \triangleq \mathbf{I} - \mathbf{A}(\mathbf{p})\mathbf{A}(\mathbf{p})^{\dagger}$ is the projector matrix of the subspace perpendicular to the Range($\mathbf{A}(\mathbf{p})$). Let $\mathbf{y}(\boldsymbol{\alpha})^{\perp} \triangleq \mathbf{P}_{\mathbf{p}}^{\perp}\mathbf{y}(\boldsymbol{\alpha})$ and $\mathbf{x}_{\mathbf{p}} \triangleq \mathbf{A}(\boldsymbol{\alpha})^{\dagger}\mathbf{y}(\boldsymbol{\alpha})$, the authors prove the following in [58]:

$$\frac{1}{2}\frac{\partial}{\partial p_i}\left\|\mathbf{P}_{\mathbf{p}}^{\perp}\mathbf{y}(\boldsymbol{\alpha})\right\|_2^2 = \left\langle \mathbf{y}(\boldsymbol{\alpha})^{\perp},\ \mathbf{A}_i\mathbf{x}_{\mathbf{p}} - \mathbf{y}_i \right\rangle, \tag{3.16}$$

which makes P_1 solvable using fast gradient based techniques such as the following:

Coordinate Gradient Descent (CGD): CGD is a gradient based algorithm to solve l_1 constrained optimization problems [59]. The following adaptation of CGD provides a solution to P_1:

Algorithm 2 CGD for P_1

$\mathbf{p}^0 \leftarrow \mathbf{0}$, $k \leftarrow 0$

while $\left\|\mathbf{p}^k - \mathbf{p}^{k-1}\right\| > \Delta$ **do**

$l \leftarrow \arg\min_i \left|\langle \mathbf{y}(\boldsymbol{\alpha})^{\perp},\ \mathbf{A}_i\mathbf{x}_{\mathbf{p}} - \mathbf{y}_i\rangle\right|$

$\mathbf{c} \leftarrow \mathbf{0}\ ,\quad \mathbf{c}_k \leftarrow -sign(< \mathbf{y}(\boldsymbol{\alpha})^{\perp},\ \mathbf{A_l}\mathbf{x_p} - \mathbf{y_l}) >$

$\hat{\lambda} \leftarrow \arg\min_{\lambda\in[0,1]} \left\|\mathbf{P}^{\perp\perp}_{\mathbf{p}\,\mathbf{p}^k+\lambda(\mathbf{c}-\mathbf{p}^k)}\mathbf{y}(\mathbf{p}^k + \lambda(\mathbf{c}-\mathbf{p}^k))\right\|_2$

$\mathbf{p}^{k+1} \leftarrow \mathbf{p} + k + \hat{\lambda}(\mathbf{c} - \mathbf{p} + k)$

$k \leftarrow k + 1$

end while

$\hat{\mathbf{A}} \leftarrow (\mathbf{A} - \sum_{i=1}^N \mathbf{A}_i p_i^k),\ \hat{\mathbf{y}} \leftarrow (\mathbf{A} - \sum_{i=1}^N \mathbf{y}_i p_i^k),\ \hat{\mathbf{x}} \leftarrow \mathbf{x}^k$

Remark 8. *The exact optimization over λ is non-convex. However it can be accurately approximated via the following:*

$$\begin{aligned}
&\arg\min_{\lambda\in[0,1]} \left\|\mathbf{P}^{\perp\perp}_{\mathbf{p}\,\mathbf{p}+\lambda(\mathbf{c}-\mathbf{p})}\mathbf{y}(\mathbf{p}+\lambda(\mathbf{c}-\mathbf{p}))\right\|_2 \\
\approx\ &\arg\min_{\lambda\in[0,1]} \|\mathbf{A}(\mathbf{p}+\lambda(\mathbf{c}-\mathbf{p}))\mathbf{x} - \mathbf{y}(\mathbf{p}+\lambda(\mathbf{c}-\mathbf{p}))\|_2 \\
=\ &\begin{cases} 0 & \alpha(\mathbf{A}^\dagger\mathbf{y}) \le 0 \\ \alpha(\mathbf{A}^\dagger\mathbf{y}) & 0 < \alpha(\mathbf{A}^\dagger\mathbf{y}) < 1 \\ 1 & \alpha(\mathbf{A}^\dagger\mathbf{y}) > 1 \end{cases}
\end{aligned}$$

$$\textit{where } \alpha(\mathbf{x}) \triangleq \frac{(\mathbf{A}(\mathbf{p})\mathbf{x} - \mathbf{y}(\mathbf{p}))^T \sum_i (\mathbf{A}_i\mathbf{x} - \mathbf{y}_i)(\mathbf{c}-\mathbf{p})}{\|\sum_i (\mathbf{A}_i\mathbf{x} - \mathbf{y}_i)(\mathbf{c}-\mathbf{p})\|_2^2}\ .$$

3.4 Numerical Results and Applications

3.4.1 Probability of Exact Recovery

For the case $\mathbf{x}_0$ is unknown, the exact recovery of perturbation may seem hopeless. However we demonstrate that exact recovery can be achieved with a high probability with the proposed estimator if the *overdetermination ratio* $\frac{m}{n}$ of the matrix is sufficiently large. A Toeplitz matrix with random elements $\mathbf{A}_0$ is perturbed by preserving the structure with k-sparse perturbations $\mathbf{p}$ and P_0 is solved to recover the perturbation. The empirical probability of exact recovery in 100 trials versus the ratio m/n is shown in Figure 3.1(a). And the probability of exact recovery is examined in the $(\frac{m}{n}, k)$ plane in Figure 3.1(b).

3.4.2 Blind Identification of Sparse Multipath Channels

Consider a channel model which consists of N_p paths with attenuations a_i, delays n_i and doppler shifts ν_i :

$$y[n] \;=\; \sum_{i=1}^{N_p} a_i x_0[n-n_i] e^{j2\pi\frac{\nu_i}{d}} + w[n] \quad , \tag{3.17}$$

which can be written more compactly as, $\mathbf{y} = \mathbf{H}\mathbf{x_0} + \mathbf{w}$, where $\mathbf{w}$ is circularly symmetric Gaussian white noise. Here we consider the joint estimation of the channel and its input following a training session that provided a channel estimate $\mathbf{H}$ with N_p paths. Since the paths are usually sparse in delay-doppler domain [60], the problem turns out to be a sparse perturbation recovery problem over a discretized delay-doppler domain with bins of length $\Delta\nu = \frac{1}{n}$, $\Delta\tau = \frac{1}{B}$ where B is the bandwidth of $x_0[n]$. To simplify the development, we define $N = md$ structure matrices as the following basis of time-frequency shifts [49]:

$$\mathbf{H}_{kl} = diag([1 \; e^{j\frac{2\pi}{d}k} \; \ldots \; e^{j\frac{2\pi}{d}km}])\mathbf{R}_l \quad , \tag{3.18}$$

where $\mathbf{R}_l$ is a matrix whose l^{th} subdiagonal entries are 1 and the rest is zero, effectively performing *shift by l* operation.

Note that $\mathbf{H}_{kl}$'s have Toeplitz structure and generate sufficiently incoherent perturbations depending on $x_0[n]$ as we outline in Remark 5. A simulation study is done to demonstrate the performance of proposed solver P_1 where $\mathbf{x}_0$ is selected as a random ± 1 sequence and assumed unknown. 1, 3 and 5 more paths with unknown attenuations, delays and doppler shifts are added respectively to a known channel $\mathbf{H}$. The parameter t is selected such that the perturbation sparsity matches the number of unknown channels. In Figures 3.2 and 3.3, the Basis Pursuit approach that we described in (3.4) where $\mathbf{x}_0$ is known is compared in terms of doppler and delay estimation error defined by $\sqrt{\frac{\nu}{d\Delta\nu}}$ and $\sqrt{\frac{\tau}{d\Delta\tau}}$ by averaging 100 realizations of noise in 30 SNR levels. Although $\mathbf{x}_0$ is unknown, the proposed scheme outperforms BP in terms of perturbation recovery and successfully estimates both the input sequence by identifying unknown paths in the channel.

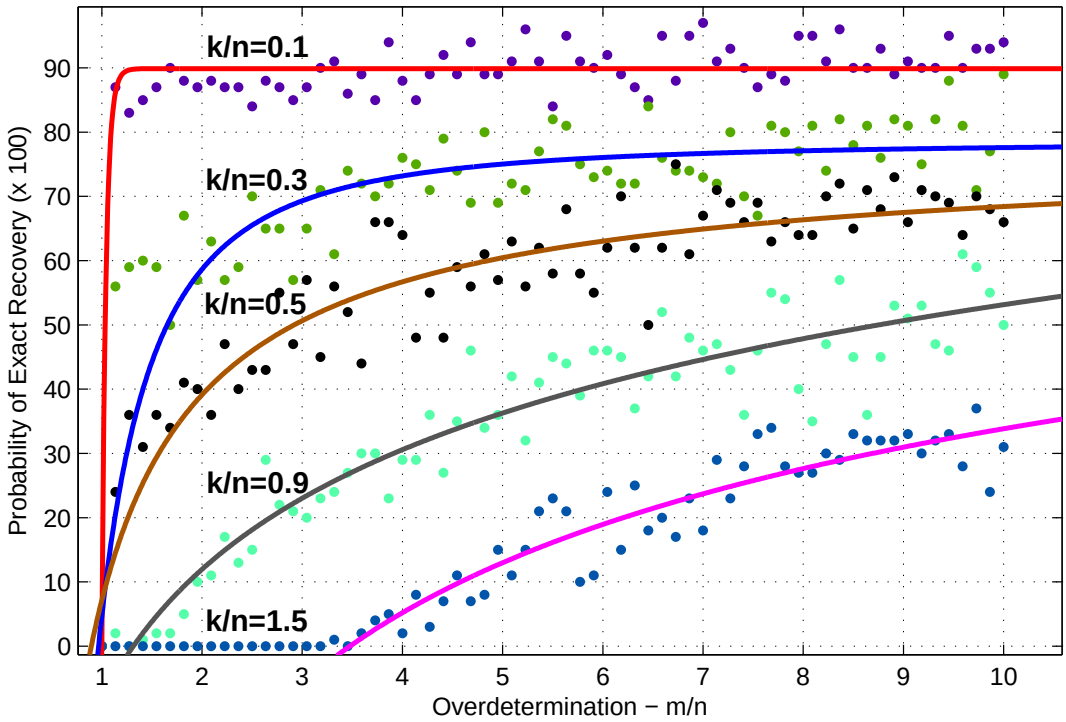

(a) Empirical probability of exact recovery versus overdetermination ratio of the proposed estimator P_0 for Toeplitz structured sparse perturbations.

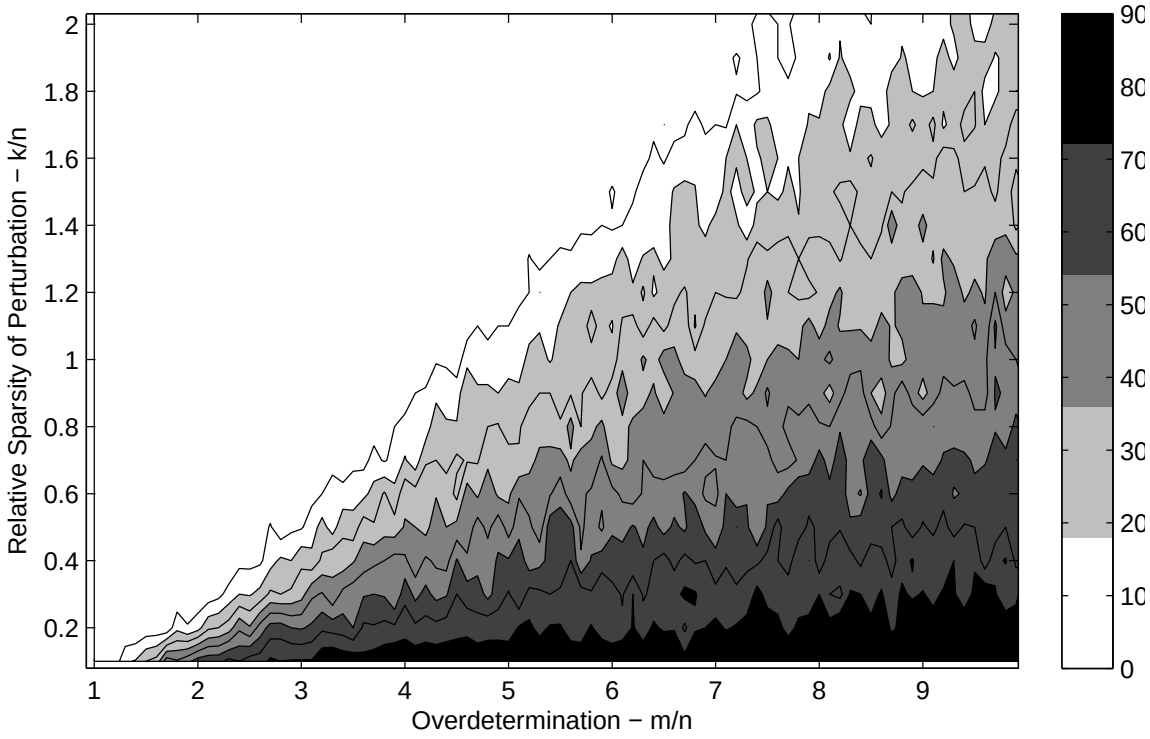

(b) Empirical probability of exact recovery in the $(\frac{m}{n}, \frac{k}{n})$ plane.

Figure 3.1: Empirical probability of exact recovery for the case where $\mathbf{x}_0$ is unknown.

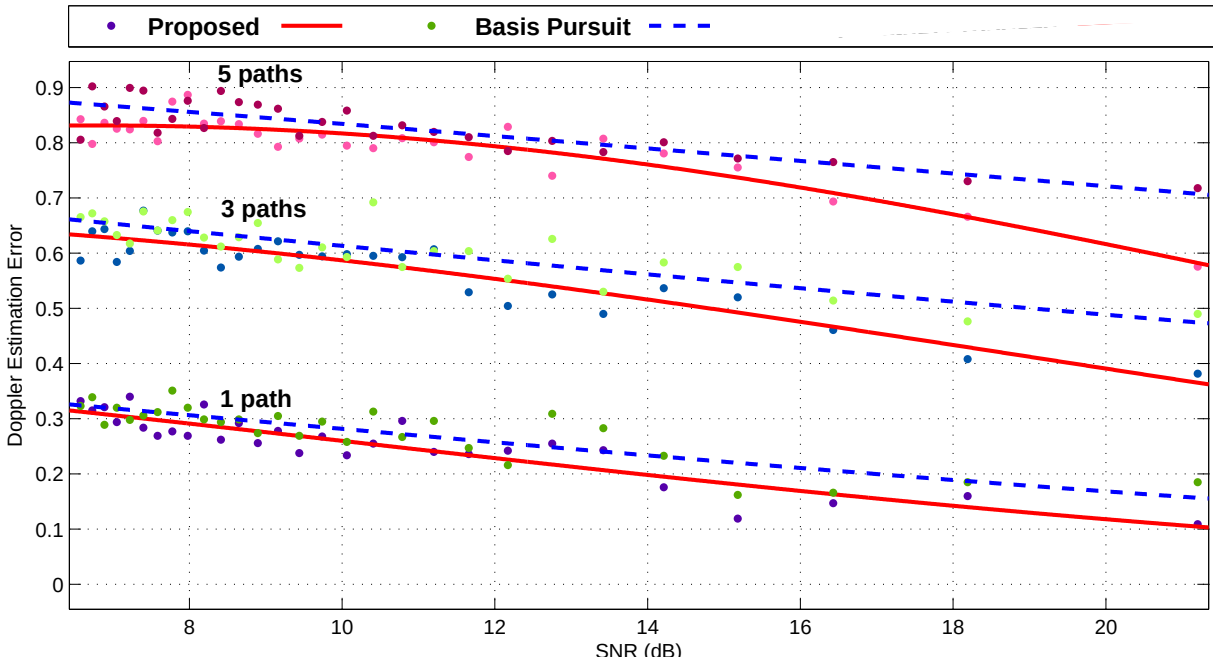

Figure 3.2: Normalized Doppler Estimation Error.

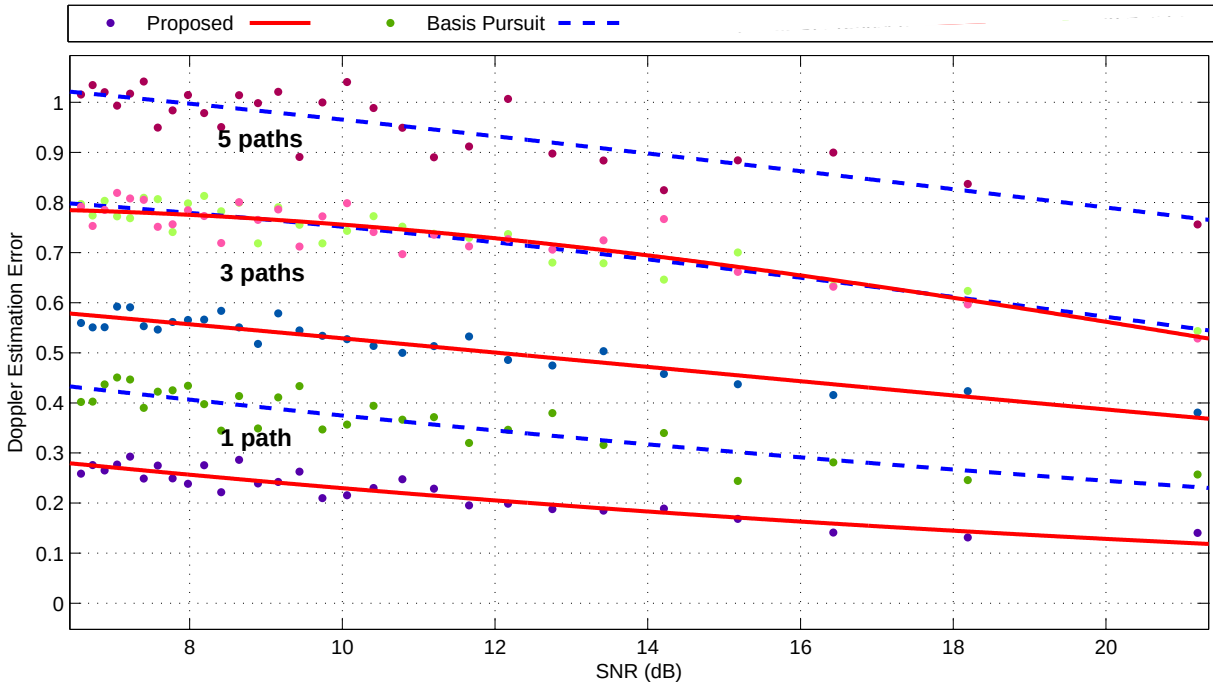

Figure 3.3: Normalized Delay Estimation Error.

Chapter 4

UNDERDETERMINED CASE: Polarization of Continuous Random Variables

4.1 Definitions and Preliminaries

4.1.1 Differential Entropy

For a random variable X with probability density function f, we define its differential entropy $H(X)$ as,

$$h(X) \triangleq -\int f \log f, \tag{4.1}$$

which measures the amount of uncertainty in the distribution of X. It is a well known fact that, for a fixed mean and variance the entropy is maximized by the Gaussian distribution, i.e.,

$$h(X) \leq \frac{1}{2} \log 2\pi e Var(X) \tag{4.2}$$

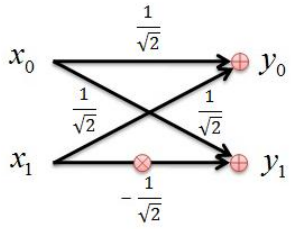

Figure 4.1: (a) Building block of the transform

with equality if and only if X is Gaussian.

The next lemma of Shannon and Stam shows that the entropy of the sum of two independent variables is at least the average of the individual entropies:

Lemma 4.1.1. *Shannon-Stam Inequality [61]*

For X, Y independent,

$$h(\frac{X+Y}{\sqrt{2}}) \geq \frac{h(X)+h(Y)}{2}. \tag{4.3}$$

with equality if and only if X and Y are Gaussian.

Now consider the circuit shown in Figure 4.1 which performs the following operation,

$$\begin{bmatrix} Y_0 \\ Y_1 \end{bmatrix} = \frac{1}{\sqrt{2}} \begin{bmatrix} 1 & 1 \\ 1 & -1 \end{bmatrix} \begin{bmatrix} X_0 \\ X_1 \end{bmatrix} \quad \text{or} \quad \mathbf{y} = \mathbf{H}_2\mathbf{x}, \tag{4.4}$$

where X_0 and X_1 are two independent identically distributed (i.i.d.) copies of the random variable X with entropy $h(X)$. The division by $\sqrt{2}$ is to ensure that the mean power at the output equals the mean power at the input. Since the transform is unitary, we have $h(\mathbf{x}) = h(\mathbf{y})$. Using chain rule for joint entropy [62] we can express this equality as,

$$h(\mathbf{x}) = 2h(X) = h(Y_0) + h(Y_1|Y_0), \tag{4.5}$$

where $h(Y_1|Y_0)$ denotes the conditional differential entropy of Y_1 given Y_0, defined as:

$$h(Y_1|Y_0) \triangleq \int_y h(Y_1|Y_0 = y) f_{Y_0}(y) dy \tag{4.6}$$

Noting that $h(Y_0) \geq h(X)$, we can rewrite (4.5) to get,

$$h(X) - h(Y_1|Y_0) = h(Y_0) - h(X). \tag{4.7}$$

The above equation states that, the entropic increase from X to Y_0 is equal to the decrease from X to $Y_1|Y_0$. The information theoretical significance of this circuit can be explained as follows: Given two i.i.d. copies of a random variable, the output is two different random objects Y_0 and $Y_1|Y_0$, one being more uncertain and the other being less uncertain than the original variable X. This phenomenon is called polarization in [63].

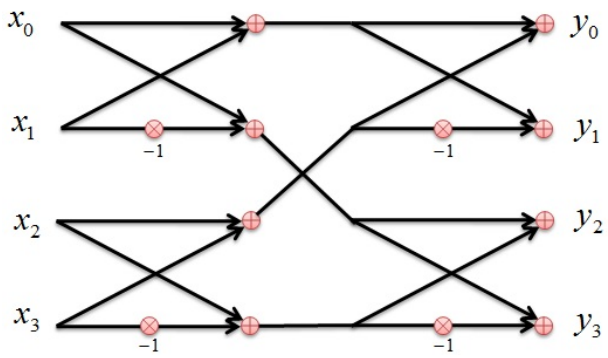

Figure 4.2: (a) Two layer application of the basic transform. (Factors of $\frac{1}{\sqrt{2}}$ are omitted from the figure.)

An important observation is that, this process can be applied in a recursive manner to obtain more uncertain and less uncertain variables in each step. Now consider Figure 4.2, which applies the same operation to the previously generated variables. Now again apply the chain rule at the output of this circuit to obtain,

$$h(\mathbf{y}) = h(Y_0) + h(Y_1|Y_0) + h(Y_1|Y_0) + h(Y_2|Y_0, Y_1) + h(Y_3|Y_0, Y_1, Y_2). \tag{4.8}$$

We now have four entropy terms compared to a single term $h(X)$ at the start of the construction. It turns out these terms show a polarization effect in some sense to be made precise in the following.

We formalize the above construction by defining recursively for each $n = 1, 2, \ldots$ the transform $\mathbf{y} = \mathbf{H}_n\mathbf{x}$ where,

$$\mathbf{y} = [Y_0, \ldots, Y_{N-1}]^T, \quad \mathbf{x} = [X_0, \ldots, X_{N-1}]^T, \quad N = 2^n \quad , \tag{4.9}$$

$$\mathbf{H}_n = \mathbf{B}\mathbf{F}^{\otimes n}, \quad \mathbf{F} = \frac{1}{\sqrt{2}} \begin{bmatrix} 1 & 1 \\ 1 & -1 \end{bmatrix} \quad . \tag{4.10}$$

$\mathbf{B}$ is an $N \times N$ permutation matrix known as the *bit reversal operation* [63], and $\mathbf{F}^{\otimes n}$ denotes the n^{th} Kronocker power of $\mathbf{F}$. Next, we consider the following conditional entropy terms in the chain rule expansion of $h(\mathbf{y})$:

$$h(\mathbf{y}) = \sum_{k=0}^{N-1} h(Y_k|Y_0, \ldots, Y_{k-1}). \tag{4.11}$$

This transform is known as the Hadamard, or the Walsh-Fourier transform in signal processing literature. Note that the analysis for the Discrete Fourier Transform is identical to the Hadamard case, since the only difference is $\pm j$ multiplications in the butterfly structure. From now on we will use the shorthand notation $h(Y_k|Y_0^{k-1})$ for $h(Y_k|Y_0, \ldots, Y_{k-1})$.

4.2 Polarizing Transform

Let, $\mathbf{y} = \mathbf{H}_n\mathbf{x} + \mathbf{n}$, where $\mathbf{x}$ is an i.i.d vector of a random variable X with $Var(X) = \sigma_x^2$, and $\mathbf{n}$ is a Gaussian vector containing i.i.d copies of $N \sim \mathcal{N}(0, \sigma_n^2)$. As described in [63], the path of the conditional entropy terms in (4.11) can be thought of as being determined by a sequence of i.i.d. Bernoulli($\frac{1}{2}$) random variables. First, define a random process E_n whose realizations are 2^n possible values of $h(Y_k|Y_0^{k-1})$, $0 \leq k \leq 2^n - 1$ at stage n with equal probability $1/2^n$. E_n is a martingale process by the observation in (4.7). Moreover, we have the following upper and lower bounds,

$$h(N) \overset{(a)}{\leq} h(Y_k|Y_0^{k-1}) \overset{(b)}{\leq} h(Y_k) \overset{(c)}{\leq} \log 2\pi e(\sigma_x^2 + \sigma_n^2) \tag{4.12}$$

where the inequalities follow from the following facts:
(a) $h(Y_k|Y_0^{k-1}) \geq h(Y_k|Y_0^{k-1}, \mathbf{x}) = h(Y_k + N_k|Y_0^{k-1}, \mathbf{x}) = h(N_k|Y_0^{k-1}, \mathbf{x}) = h(N_k)$.
(b) Conditioning on other variables does not increase entropy.
(c) Follows from Equation (4.2).
Therefore E_n is a bounded martingale. Then the Theorem 9.4.6 of [64] implies that the sequence of random variables $\{E_n; n \geq 0\} \rightarrow E_\infty$ a.e. where $E[E_\infty] = E[E_0]$.

The next lemma shows that the average of the conditional entropy terms is equal to $h(X + N)$.

Lemma 4.2.1.

$$\textit{For any } N, \quad \frac{1}{N}\sum_{k=0}^{N-1} h(Y_k|Y_0^{k-1}) = h(X + N). \tag{4.13}$$

Proof:

Note that the transform $\mathbf{y} = \mathbf{H}_n\mathbf{x}+\mathbf{n}$ can also be written as $\mathbf{y} = \mathbf{H}_n(\mathbf{x}+\tilde{\mathbf{n}})$ where $\tilde{\mathbf{n}}$ is statistically equivalent to $\mathbf{n}$ since $\mathbf{H}_n$ is unitary. Then, $h(\mathbf{y}) = h(\mathbf{x} + \tilde{\mathbf{n}}) = Nh(X + N)$. Using the chain rule to expand $h(\mathbf{y})$ proves the result. ■

The next lemma states the condition under which the entropy strictly increases in recursive application of the butterfly structure.

Lemma 4.2.2. , *Given random variables Y_0, Y_1, Y_2, Y_3 with joint distribution $f_{Y_0,Y_1,Y_2,Y_3}(y_0, y_1, y_2, y_3) = f_{Y_0,Y_1}(y_0, y_1)f_{Y_2,Y_3}(y_2, y_3)$,*

$$h(\frac{Y_1 + Y_3}{\sqrt{2}}|Y_0, Y_2) \geq \frac{1}{2}\Bigg(h(Y_1|Y_0) + h(Y_3|Y_2)\Bigg), \tag{4.14}$$

with equality if and only if $f_{Y_1|Y_0=y_0}$ and $f_{Y_3|Y_2=y_2}$ are Gaussian and $h(Y_1|Y_0 = y_0) = h(Y_3|Y_2 = y_2) \ \ \forall y_0, y_2$.

Proof:

The Entropy Power Inequality [61] states that, for two independent random

variables X, Y,

$$e^{2H(X+Y)} \geq e^{2H(X)} + e^{2H(Y)} \tag{4.15}$$

with equality if and only if both X and Y are Gaussian. By simple algebraic manipulations we get:

$$h(\frac{X+Y}{\sqrt{2}}) \geq \frac{1}{2}\log\left(\frac{e^{2h(X)} + e^{2h(Y)}}{2}\right). \tag{4.16}$$

By the strict concavity of the logarithm,

$$\begin{aligned} h(\frac{X+Y}{\sqrt{2}}) &\geq \frac{1}{2}\left(\frac{1}{2}\log(e^{2h(X)}) + \frac{1}{2}\log(e^{2h(Y)}\right) && (4.17)\\ &= \frac{1}{2}\left(h(X) + h(Y)\right) && (4.18) \end{aligned}$$

with equality if and only if $h(X) = h(Y)$ and X, Y Gaussian. Now, returning to the original variables,

$$\begin{aligned} h(\frac{Y_1+Y_3}{\sqrt{2}}|Y_0, Y_2) &= \int_{y_0}\int_{y_2} h(\frac{Y_1+Y_3}{\sqrt{2}}|Y_0 = y_0, Y_2 = y_2) f_{Y_0,Y_2}(y_0, y_2)dy_0dy_2 \\ &\geq \int_{y_0}\int_{y_2} \frac{h(Y_1|Y_0 = y_0) + h(Y_3|Y_2 = y_2)}{2} f_{Y_0,Y_2}(y_0, y_2)dy_0dy_2 \\ &= \frac{1}{2}\left(\int_{y_0} h(Y_1|Y_0 = y_0)f_{Y_0}(y_0)dy_0 + \int_{y_2} h(Y_3|Y_2 = y_2)f_{Y_2}(y_2)dy_2\right) \\ &= \frac{1}{2}\left(h(Y_1|Y_0) + h(Y_3|Y_2)\right) \end{aligned}$$

with equality if and only if, $f_{Y_1|Y_0=y_0}$ and $f_{Y_3|Y_2=y_2}$ are Gaussian and $h(Y_1|Y_0 = y_0) = h(Y_3|Y_2 = y_2) \ \ \forall y_0, y_2$. ■

Therefore, as long as the conditional distributions are non-Gaussian in the n^{th} stage, there will be increases and decreases in conditional entropy terms from n^{th} stage to $(n+1)^{th}$ stage. We now present a bound on conditional entropy terms which is asymptotically tight.

Theorem 4.2.3.

$$\textit{For any } k, \quad h(Y_k|Y_0^{k-1}) \leq \frac{1}{2}\log 2\pi e E[Var(Y_k|Y_0^{k-1})], \tag{4.19}$$

and the equality condition is satisfied asymptotically $\forall k$.

Proof:

$$
\begin{aligned}
h(Y_k|Y_0,\ldots,Y_{k-1}) &= \int h(Y_k|Y_0^{k-1}=y_0^{k-1})p(y_0^{k-1})dy_0^{k-1} && (4.20)\\
&\overset{(a)}{\leq} \int\left[\frac{1}{2}\log 2\pi eVar(Y_k|Y_0^{k-1}=y_0^{k-1})\right]p(y_0^{k-1})dy_0^{k-1}\\
&\overset{(b)}{\leq} \frac{1}{2}\log 2\pi e\int Var(Y_k|Y_0^{k-1}=y_0^{k-1})]p(y_0^{k-1})dy_0^{k-1}\\
&= \frac{1}{2}\log 2\pi eE[Var(Y_k|Y_0,\ldots,Y_{k-1})] && (4.21)
\end{aligned}
$$

where the inequalities follow from the following facts:

(a) Gaussians maximize entropy for a fixed variance,

(b) strict concavity of the logarithm and Jensen's Inequality.

We have equality in (a) if and only if Y_k is conditionally Gaussian given $Y_0^{k-1}=y_0^{k-1}$ for each y_0^{k-1}, and equality in (b) if and only if $Var(Y_k|Y_0^{k-1}=y_0^{k-1})$ is independent of y_0^{k-1}. Next, note that by the Martingale argument, the process converges to a limiting distribution. The convergence of the process E_n implies that, the equality conditions of Lemma 4.2.2 are asymptotically satisfied, which in turn implies the equality conditions in the above set of inequalities. ■

The previous theorem shows that the conditional entropy terms can not polarize to a binary valued limiting random variable as in the finite field case. The conditional entropy terms are bounded by Gaussian entropies corresponding their expected conditional variances. A simple corollary of this result is the following limit on the expected variances:

Lemma 4.2.4.

$$\lim_{N\to\infty}\left[\prod_{k=0}^{N-1}2\pi eE[Var(Y_k|Y_0^{k-1})]\right]^{\frac{1}{N}} = e^{2h(X+N)}. \qquad (4.22)$$

Proof:

Using the result of Theorem 4.2.3 in Lemma 4.2.1 we have,

$$\lim_{N\to\infty} \frac{1}{N} \sum_{k=0}^{N-1} \frac{1}{2} \log 2\pi e E[Var(Y_k|Y_0^{k-1})] = h(X+N). \tag{4.23}$$

which is equivalent to (4.22) by the continuity of the logarithm.

The next lemma will demonstrate that if k is a power of two then $h(Y_k|Y_0^{k-1})$ converges to the upper bound .

Lemma 4.2.5. *Let $k = 2^i$ for some $i \geq 0$. Then,*

$$E[Var(Y_k|Y_0, \ldots, Y_{k-1})] = \sigma_x^2 + \sigma_n^2. \tag{4.24}$$

Proof:

Using the Law of Total Variance we have,

$$E[Var(Y_k|Y_0, \ldots, Y_{k-1})] + Var(E[Y_k|Y_1, \ldots, Y_{k-1}]) = Var(Y_k) = \sigma_x^2 + \sigma_n^2. \tag{4.25}$$

For any $r > 0$, we have the following property by the recursive construction:

$$\begin{aligned} Var(E[Y_{2r}|Y_1, \ldots, Y_{2r-1}]) &= Var\left(E\left[\frac{U_r + V_r}{\sqrt{2}}|Y_1, \ldots, Y_{2r-1}\right]\right) & (4.26) \\ &= Var(E[U_r|U_1, \ldots, U_{r-1}], & (4.27) \end{aligned}$$

where U and V are the variables of the previous layer whose sum constructs the variables at the output layer. Since k is a power of 2, we can apply the above reduction formula till we reach the input variables $\mathbf{x}$ and we get,

$$Var(E[Y_k|Y_1, \ldots, Y_{k-1}]) = Var(E[X_1|X_0]) = 0, \tag{4.28}$$

where the last equality follows from the fact taht $E[X_1|X_0]$ is equal to zero with probability 1. Then we have $E[Var(Y_k|Y_1, \ldots, Y_{k-1})] = \sigma_x^2 + \sigma_n^2$. ■

Therefore, the terms with power of two indices have expected variance $\sigma_x^2 + \sigma_n^2$ and converge to the upper bound $\frac{1}{2} \log 2\pi e(\sigma_x^2 + \sigma_n^2)$.

We also conjecture that, infinitely many conditional terms should converge to the lower bound $h(N)$. This can be verified by working on a given distribution. For example, when X has a memoryless distribution the analysis is tractable. However we conclude that the polarization phenomenon in the continuous case is slightly different than the finite field case since the conditional entropy terms converge to Gaussian entropies with a spectrum of variances.

4.3 Polar Sampling

Let $\mathbf{x} \in \mathbb{R}^N$ be a signal which is composed of i.i.d copies of a *compressible*, i.e., low entropy random variable X. First apply the polarizing transform $\mathbf{H}_n$,

$$\mathbf{y} = \mathbf{H}_n \mathbf{x} + \mathbf{n} \ . \tag{4.29}$$

For a highly compressible X, we expect that many conditional entropy terms in the expansion,

$$\sum_{k=0}^{N-1} h(Y_k | Y_1, \ldots, Y_{k-1}) = N h(X+N), \tag{4.30}$$

converge to the lower bound $h(N)$. The following numerical example shows that this is the case. An i.i.d random vector containing copies of $U[-a,a]$ is applied to the $\mathbf{H}_n$ and the conditional entropy $h(Y_k|Y_1,\ldots,Y_{k-1}) = h(Y_1 \ldots, Y_k) - h(Y_1 \ldots, Y_{k-1})$ is estimated using Kozachenko- Leonenko entropy estimator [65].

Therefore a high entropy subset of the output variables $\mathbf{y}$ are sufficient to recover the whole vector $\mathbf{y}$, hence the unknown $\mathbf{x}$ to the linear equations. In the next example, we demonstrate the recovery of a low entropy signal by sampling only high-entropy rows, which correspond to high conditional entropy terms, of its Hadamard transform and compare with Compressed Sensing.

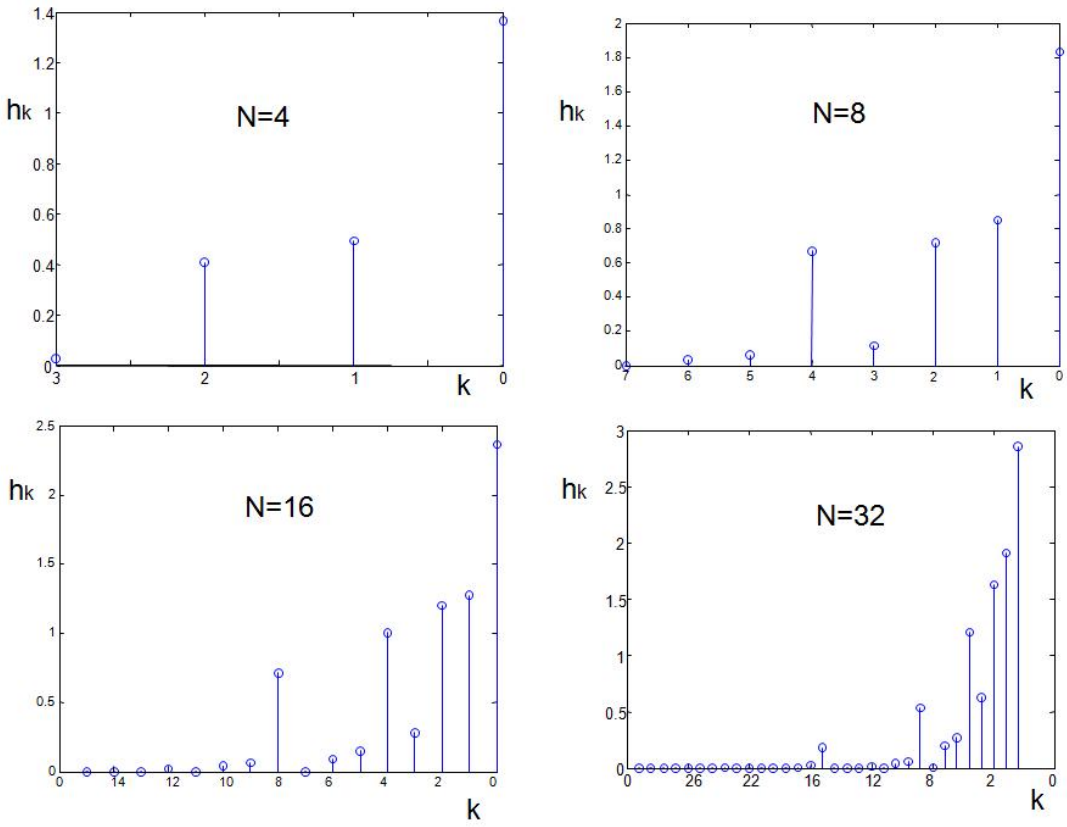

(a) Empirical Distribution of Conditional Entropies

The signal shown in Figure 4.3(b) is a piecewise polynomial signal of the following form,

$$s[n] = a_i n^3 + b_i n^2 + c_i n + d_i, \quad 1 \leq n_i \leq n \leq n_{i+1} \leq 2048$$

and those signals are known to be sparse in the Daubechies-8 wavelet basis, hence compressible. The transform domain wavelet coefficients are shown in Figure 4.3(c). The length 2048 signal is compressively sampled using 600 inner products both using a random Gaussian matrix and a Hadamard matrix. For the Hadamard matrix, only the high-entropy indices corresponding to high $h(Y_k|Y_1^{k-1})$ values are sampled. Those high indices of the Hadamard matrix are calculated beforehand by the KL entropy estimator. In both cases the recovery is done using Basis Pursuit DeNoising (BPDN) of Sparco Toolbox [66] and compared in Figure 4.3(d) and 4.3(e).

The reconstruction using the high entropy rows of the Hadamard matrix show superior performance compared to random Gaussian sampling using less number of wavelet coefficients. This result is a simple demonstration of the practical performance of a high entropy sampling approach. It should also be noted that, the main advantage of random Gaussian sampling is its universality. In order to use the Polar Sampling approach, the high entropy rows should be calculated beforehand. We also conjecture that the order in which the conditional entropies are distributed asymptotically is universal and independent from source distribution. Therefore there may be no need to recalculate the order of conditional entropies.

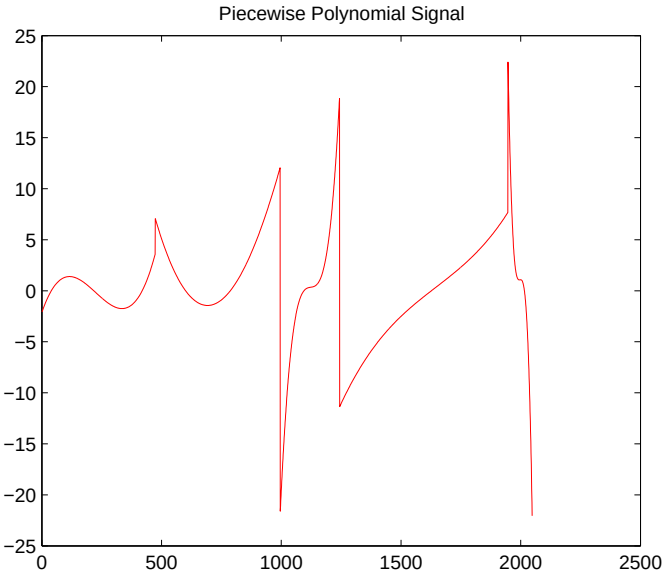

(b) Piecewise polynomial signal

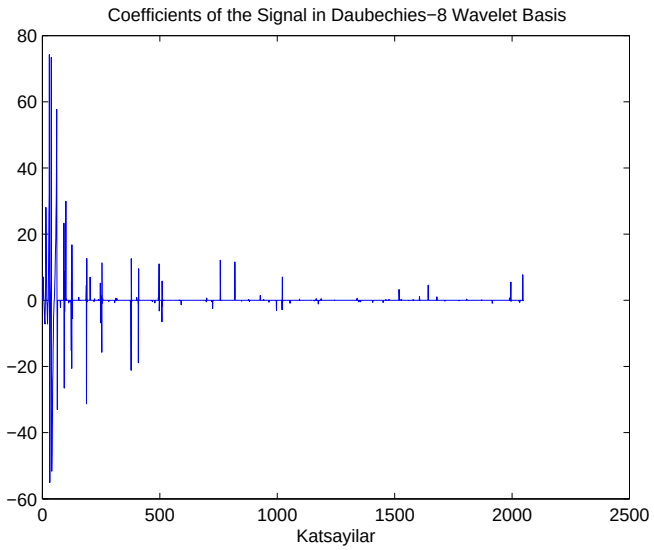

(c) Coefficients of the signal in Daubechies-8 wavelet basis

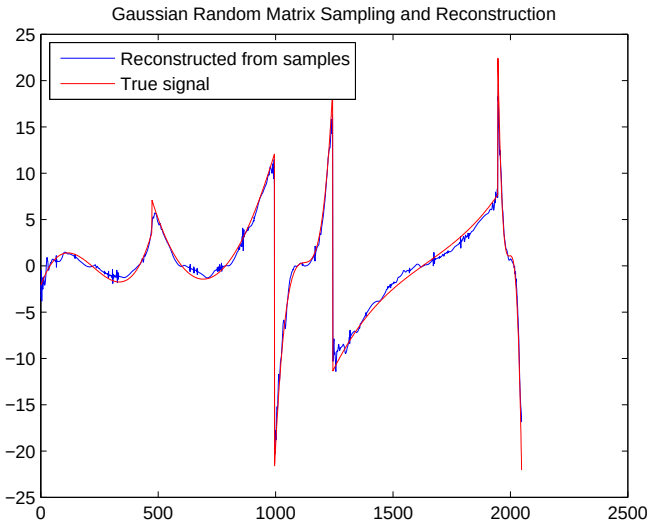

(d) Compressed Sensing using a random Gaussian matrix and recovery using **175** terms

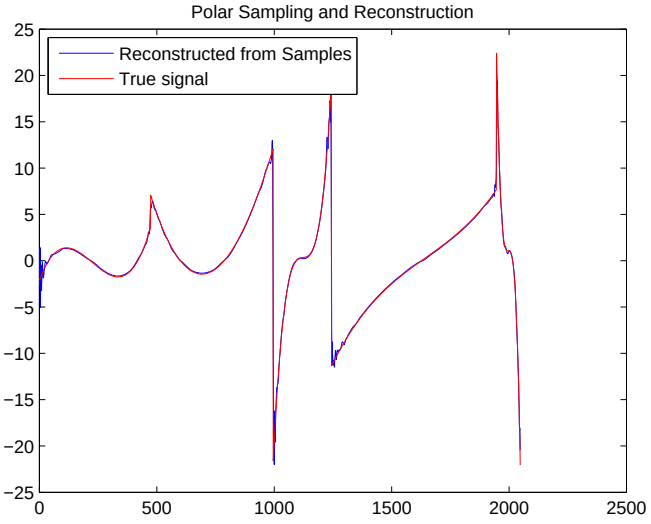

(e) Polar Sampling and Recovery using **140** terms

Figure 4.3: Sub-Nyquist sampling and recovery of a piecewise polynomial signal

Chapter 5

CONCLUSIONS

In this thesis we presented theoretical and practical results on linear equations with uncertainty. In the first part, the case in which the number of equations exceeds the number of unknowns is considered. The main focus was on linear regression problems with possibly structured uncertainty in all variables. A novel estimator, SLS-BDU is proposed in terms of a non-convex optimization problem. The analysis of the MSE of the SLS-BDU estimator reveals the advantage over the alternative estimators. We derived sufficient conditions where the proposed estimator improves upon the conventional estimate. Three different methods are presented for iterative solution of the optimization problem. Among the three methods, the Fréchet gradient approach provides the fastest convergence. Furthermore, the gradient flow space enables us to study alternative approaches and be able to compare their performances. New theorems that characterize the gradient flow for practical cases of interest are proven. A simple but efficient criterion to select the optimization parameter based on the gradient norm is proposed. Extensive comparison results on the SLS-BDU estimator reveal the superior performance of the proposed technique in signal restoration, multiple frequency estimation and system identification applications. The automated selection of the optimization parameter adaptively regularizes the solution based

on SNR and achieves improved MSE compared to the notable alternative RSTLS technique.

An important special case of uncertainty in the overdetermined case is when uncertainty is sparse in some basis. We showed that the exact or stable recovery of sparse perturbations in Least Squares problems is achievable under some conditions. It is found that, ill-conditioning of the matrix and coherence of perturbations are the limitations of recovery of a sparse uncertainty. We proposed an optimization scheme and its convex relaxation to recover the uncertainty and the solution jointly. The numerical examples show that the empirical probability of exact recovery is very high for reasonable overdetermination ratios and it has superior performance in practice when applied to identification of sparse multipath channels.

The second part is on the recovery of the solution when the number of equations is less than the number of unknowns. We took an information theoretical approach and exhibited a special matrix which enables the recovery of unknowns from few equations. Our results are a generalization of source/channel polarization theory for continuous distributions and not limited to solving linear equations. Theoretical results on the evolution of conditional entropies are presented. We showed that, the Hadamard matrix and Discrete Fourier Transform matrix, can be used to capture the entropy of a compressible i.i.d vector from few inner products. The performance of the method is compared with Compressed Sensing in a numerical example where we sample and reconstruct a low dimensional signal.

APPENDIX A

Singularity of the Fisher Information Matrix

It is known that for a singular Fisher information matrix, there exists no unbiased estimator with finite variance except under unusual circumstances [67]. In the following proof, we show that the information matrix is singular for the deterministic perturbation case when $p > m - n$.

Proof: The observation $\mathbf{y}$ is related to unknowns $\mathbf{x}$ and $\boldsymbol{\theta}$ as,

$$\mathbf{y} = \mathbf{A}_0\mathbf{x} + \sum_i \mathbf{y}_i\boldsymbol{\theta}_i + \mathbf{w} = (\mathbf{A} - \sum_i \mathbf{A}_i\boldsymbol{\theta}_i)\mathbf{x} + \sum_i \mathbf{y}_i\boldsymbol{\theta}_i + \mathbf{w}.$$

Define $\mathbf{A}_{\boldsymbol{\theta}} \triangleq (\mathbf{A} - \sum_i \mathbf{A}_i\boldsymbol{\theta}_i)$ and $\mathbf{B} \triangleq [\mathbf{y}_1, ..., \mathbf{y}_p]$. Given that $\mathbf{w}$ is a zero mean Gaussian random vector with covariance $\sigma^2\mathbf{I}$, the log-likelihood can be written as:

$$\log p_{\boldsymbol{\theta}}(\mathbf{y}) = -\frac{m}{2}\log 2\pi - m\log\sigma - \frac{1}{2\sigma^2}\left\|\mathbf{y} - (\mathbf{A}_{\boldsymbol{\theta}}\mathbf{x} + \mathbf{B}\boldsymbol{\theta})\right\|_2^2.$$

Defining the vector of unknowns $\mathbf{z} \triangleq \begin{bmatrix} \mathbf{x} \\ \boldsymbol{\theta} \end{bmatrix}$ and $\mathbf{Q} \triangleq [\mathbf{A}_1\mathbf{x}, ..., \mathbf{A}_p\mathbf{x}]$, the gradient of the log-likelihood can be obtained as:

$$\frac{\partial}{\partial \mathbf{z}} p_{\boldsymbol{\theta}}(\mathbf{y}) = \frac{-1}{\sigma^2}\begin{bmatrix} \mathbf{A}_{\boldsymbol{\theta}}^T(\mathbf{A}_{\boldsymbol{\theta}}\mathbf{x} + \mathbf{B}\boldsymbol{\theta} - \mathbf{y}) \\ (\mathbf{B} - \mathbf{Q})^T(\mathbf{A}_0\mathbf{x} - \mathbf{Q}\boldsymbol{\theta} + \mathbf{B}\boldsymbol{\theta} - \mathbf{y}) \end{bmatrix}.$$

and the corresponding Fisher Information Matrix can be expressed as:

$$\begin{aligned}
\mathbf{I}_{\mathbf{x},\boldsymbol{\theta}} &= E\left[\frac{\partial}{\partial \mathbf{z}} p_{\boldsymbol{\theta}}(\mathbf{y}) \left(\frac{\partial}{\partial \mathbf{z}} p_{\boldsymbol{\theta}}(\mathbf{y})\right)^T\right] \\
&= \frac{1}{\sigma^4} E \begin{bmatrix} \mathbf{A}_{\boldsymbol{\theta}}^T \mathbf{w}\mathbf{w}^T \mathbf{A}_{\boldsymbol{\theta}} & \mathbf{A}_{\boldsymbol{\theta}} \mathbf{w}\mathbf{w}^T (\mathbf{B}-\mathbf{Q}) \\ (\mathbf{B}-\mathbf{Q})^T \mathbf{w}\mathbf{w}^T \mathbf{A}_{\boldsymbol{\theta}} & (\mathbf{B}-\mathbf{Q})^T \mathbf{w}\mathbf{w}^T (\mathbf{B}-\mathbf{Q}) \end{bmatrix} \\
&= \frac{1}{\sigma^2} \begin{bmatrix} \mathbf{A}_{\boldsymbol{\theta}}^T \mathbf{A}_{\boldsymbol{\theta}} & \mathbf{A}_{\boldsymbol{\theta}} (\mathbf{B}-\mathbf{Q}) \\ (\mathbf{B}-\mathbf{Q})^T \mathbf{A}_{\boldsymbol{\theta}} & (\mathbf{B}-\mathbf{Q})^T (\mathbf{B}-\mathbf{Q}) \end{bmatrix}.
\end{aligned}$$

Next we use the following fact, assume $\mathbf{A}_{11}$ is invertible, the block matrix

$$\begin{bmatrix} \mathbf{A}_{11} & \mathbf{A}_{12} \\ \mathbf{A}_{21} & \mathbf{A}_{22} \end{bmatrix}$$

is invertible if and only if $\mathbf{A}_{22} - \mathbf{A}_{21}\mathbf{A}_{11}^{-1}\mathbf{A}_{12}$ is invertible. Since we assumed $\mathbf{A}_0^T \mathbf{A}_0 = \mathbf{A}_{\boldsymbol{\theta}}^T \mathbf{A}_{\boldsymbol{\theta}}$ is invertible, $\mathbf{I}_{\mathbf{x},\boldsymbol{\theta}}$ is invertible if and only if:

$$\det\left[(\mathbf{B}-\mathbf{Q})^T(\mathbf{B}-\mathbf{Q}) - (\mathbf{B}-\mathbf{Q})^T \mathbf{A}_{\boldsymbol{\theta}} (\mathbf{A}_{\boldsymbol{\theta}}^T \mathbf{A}_{\boldsymbol{\theta}})^{-1} \mathbf{A}_{\boldsymbol{\theta}}^T (\mathbf{B}-\mathbf{Q})\right] \ ,$$

is nonzero. By using $\mathbf{P}_{\boldsymbol{\theta}}^{\perp} \triangleq \mathbf{I} - \mathbf{A}_{\boldsymbol{\theta}} (\mathbf{A}_{\boldsymbol{\theta}}^T \mathbf{A}_{\boldsymbol{\theta}})^{-1} \mathbf{A}_{\boldsymbol{\theta}}^T$, this condition can be simplified to:

$$\det\left[(\mathbf{B}-\mathbf{Q})^T \mathbf{P}_{\boldsymbol{\theta}}^{\perp} (\mathbf{B}-\mathbf{Q})\right] \neq 0$$

Therefore $\mathbf{I}_{\mathbf{x},\boldsymbol{\theta}}$ is invertible if and only if $\mathbf{P}_{\boldsymbol{\theta}}^{\perp}(\mathbf{B}-\mathbf{Q}) \in \mathbb{R}^{m \times p}$ is full column rank. Since $\mathrm{Rank}(\mathbf{P}_{\boldsymbol{\theta}}^{\perp}) = m - \mathrm{Rank}(\mathbf{A}_{\boldsymbol{\theta}})$ it is easy to show that:

$$\begin{aligned}
\mathrm{Rank}(\mathbf{P}_{\boldsymbol{\theta}}^{\perp}(\mathbf{B}-\mathbf{Q})) &\leq \min\Big\{\mathrm{Rank}(\mathbf{P}_{\boldsymbol{\theta}}^{\perp}), \mathrm{Rank}(\mathbf{B}-\mathbf{Q})\Big\} \\
&\leq m - n
\end{aligned}$$

which implies that $\mathbf{I}_{\mathbf{x},\boldsymbol{\theta}}$ is not invertible for $p > m - n$ and hence there exists no unbiased estimator with finite variance.

APPENDIX B

Proof of Theorem 2.3.2

Proof: First, for any $\beta \in \mathbb{R}_p$, the following bounds can be obtained:

$$\begin{aligned} \left\| \sum_i \mathbf{A}_i \beta_i \right\|_2^2 &\leq \left(\sum_i \|\mathbf{A}_i\|_2 \, |\beta_i| \right)^2 \leq \max_i \|\mathbf{A}_i\|_2^2 \, \|\beta\|_1^2 \\ &\leq p \max_i \|\mathbf{A}_i\|_2^2 \, \|\beta\|_2^2 \end{aligned} \tag{B.1}$$

And for nonoverlapping structures, i.e., $\mathbf{A}_i \odot \mathbf{A}_j = 0 \ , \ \forall i \neq j$:

$$\begin{aligned} \left\| \sum_i \mathbf{A}_i \beta_i \right\|_2^2 \leq \left\| \sum_i \mathbf{A}_i \beta_i \right\|_F^2 &= \sum_i \|\mathbf{A}_i\|_F^2 \, \beta_i^2 \\ &\leq \max_i \|\mathbf{A}_i\|_F^2 \, \|\beta\|_2^2 \quad . \end{aligned} \tag{B.2}$$

In particular Toeplitz and Hankel structures are nonoverlapping and both have $\max_i \|\mathbf{A}_i\|_F^2 = n$. Next we use the bound $\|\alpha\|_2 \leq \rho$ of SLS-BDU and Weyl's Theorem [68] and get:

$$\frac{1}{\sigma_{\boldsymbol{\alpha}^*}^2} \leq \frac{1}{(\sigma_A - \|\sum_i \mathbf{A}_i \alpha_i\|_2)_+^2} \leq \frac{1}{(\sigma_A - \rho S)_+^2} \quad . \tag{B.3}$$

Also observe that,

$$\|\mathbf{A}(\boldsymbol{\alpha}^*) - \mathbf{A}_0)\|_2^2 = \left\| \sum_i \mathbf{A}_i (\alpha_i + \theta_i) \right\|_2^2 \leq (\rho + \|\theta\|)^2 S^2 \tag{B.4}$$

Using (B.4) and (B.3) in Theorem 2.3.1 another MSE bound of SLS-BDU can be stated as follows:

$$E[\|\hat{\mathbf{x}} - \mathbf{x}\|_2^2] \leq \frac{(\rho + \|\theta\|)^2 S^2 \, \|\mathbf{x}_0\|_2^2 + n\sigma_w^2}{(\sigma_A - \rho S)_+^2} \quad . \tag{B.5}$$

Since STLS is an ML estimator it is asymptotically unbiased and the asymptotic MSE is equivalent to the second part of (2.23) when $\mathbf{A}(\boldsymbol{\alpha}^*)$ is replaced by $\mathbf{A}_0$:

$$E[\|\mathbf{x}_{STLS} - \mathbf{x}\|_2^2] = \sigma_w^2 \|\mathbf{A}_0\|_F^2 = \sum_{i=1}^{n} \frac{\sigma_{\mathbf{w}}^2}{\sigma_{\mathbf{A}_0,i}^2} > \frac{\sigma_w^2}{\sigma_0^2} \tag{B.6}$$

Therefore, when (2.25) is satisfied, we get,

$$E[\|\mathbf{x}_{STLS} - \mathbf{x}\|_2^2] > E[\left\|\mathbf{x}_{SLS-BDU(\rho)} - \mathbf{x}\right\|_2^2] \quad ,$$

asymptotically.

APPENDIX C

Local Lipschitz Continuity

Proposition C.0.1. *Assume* $\mathbf{A}(\boldsymbol{\alpha})$ *is of full column rank and* $\left\|\mathbf{P}_{\boldsymbol{\alpha}}^{\perp}\mathbf{y}\right\| \neq 0$ *for* $\|\mathbf{W}\boldsymbol{\alpha}\| \leq \rho$, *then* $\mathbf{f}(\boldsymbol{\alpha}) \triangleq \nabla_{\boldsymbol{\alpha}} \left\|\mathbf{P}_{\boldsymbol{\alpha}}^{\perp}\mathbf{y}\right\|_{\mathbf{2}}^{\mathbf{2}}$ *is locally Lipschitz continuous.*

Proof: Let $\alpha, \quad \beta \in \mathbb{R}^p$ be any two vectors satisfying $\text{Rank}(\mathbf{A}(\boldsymbol{\alpha})) = \text{Rank}(\mathbf{A}(\boldsymbol{\beta}))$. And let σ_{min} be the minimum singular value of $\mathbf{A}(\boldsymbol{\alpha})$ in $\|\mathbf{W}\boldsymbol{\alpha}\| \leq \rho$. Using Lemma 2.5.1 we get:

$$\|\mathbf{f}(\boldsymbol{\alpha}) - \mathbf{f}(\boldsymbol{\beta})\|_2^2 \tag{C.1}$$

$$\leq 4\sum_i (\mathbf{y}^T\mathbf{y})^2 \left\|\mathbf{P}_{\boldsymbol{\alpha}}^{\perp}\mathbf{A}_i\mathbf{A}(\boldsymbol{\alpha})^{\dagger} - \mathbf{P}_{\boldsymbol{\beta}}^{\perp}\mathbf{A}_i\mathbf{A}(\boldsymbol{\beta})^{\dagger}\right\|_2^2 \tag{C.2}$$

$$= 4\|y\|_2^4 \sum_i \left\| \frac{1}{2}\Big((\mathbf{P}_{\boldsymbol{\alpha}}^{\perp} - \mathbf{P}_{\boldsymbol{\beta}}^{\perp})\mathbf{A}_i(\mathbf{A}(\boldsymbol{\alpha})^{\dagger} + \mathbf{A}(\boldsymbol{\beta})^{\dagger}) \right.$$

$$\left. +(\mathbf{P}_{\boldsymbol{\alpha}}^{\perp} + \mathbf{P}_{\boldsymbol{\beta}}^{\perp})\mathbf{A}_i(\mathbf{A}(\boldsymbol{\alpha})^{\dagger} - \mathbf{A}(\boldsymbol{\beta})^{\dagger}) \Big) \right\|_2^2 \tag{C.3}$$

Now let $M^+ \triangleq \max(\|\mathbf{A}(\boldsymbol{\alpha})\|_2, \left\|\mathbf{A}(\boldsymbol{\beta})^{\dagger}\right\|_2)$ and $M^- \triangleq \min(\|\mathbf{A}(\boldsymbol{\alpha})\|_2, \left\|\mathbf{A}(\boldsymbol{\beta})^{\dagger}\right\|_2)$. In [55], the following are derived for pseudoinverses and projectors having the same rank:

$$\left\|\mathbf{A}(\boldsymbol{\alpha})^{\dagger} - \mathbf{A}(\boldsymbol{\beta})^{\dagger}\right\| \leq 3M^+ \|\mathbf{A}(\boldsymbol{\alpha}) - \mathbf{A}(\boldsymbol{\beta})\| \tag{C.4}$$

$$\left\|\mathbf{P}_{\boldsymbol{\alpha}}^{\perp} - \mathbf{P}_{\boldsymbol{\beta}}^{\perp}\right\| \leq M^- \|\mathbf{A}(\boldsymbol{\alpha}) - \mathbf{A}(\boldsymbol{\beta})\| \tag{C.5}$$

Using the above bounds with (B.1) yields that $\nabla_{\boldsymbol{\alpha}} \left\| \mathbf{P}_{\boldsymbol{\alpha}}^{\perp} \mathbf{y} \right\|_2^2$ is Lipschitz continuous with constant:

$$\begin{aligned} \|y\|_2^2 \, S(3M^+ \left\| \mathbf{P}_{\boldsymbol{\alpha}}^{\perp} + \mathbf{P}_{\boldsymbol{\beta}}^{\perp} \right\| + M^- \left\| \mathbf{A}(\boldsymbol{\alpha})^{\dagger} + \mathbf{A}(\boldsymbol{\beta})^{\dagger} \right\|_2) \\ \leq 2 \|y\|_2^2 \, S\left(\frac{1}{\sigma_{min}^2} + \frac{3}{\sigma_{min}} \right) \end{aligned} \tag{C.6}$$

Using the above result, we will next prove that the Algorithm 3 converges geometrically provided that ρ is sufficiently small:

Theorem C.0.2. *If ρ satisfies:*

$$2\rho\kappa \|y\|_2^2 \, S \leq \frac{\sigma_{min}^2}{1 + 3\sigma_{min}} \min_{\|\mathbf{W}\boldsymbol{\alpha} \leq \rho\|} \|\mathbf{W}\mathbf{f}(\boldsymbol{\alpha})\|_2 \quad , \tag{C.7}$$

where $\kappa \triangleq \|\mathbf{W}\|_2 \left\| \mathbf{W}^{\dagger} \right\|_2$ is the condition number of $\mathbf{W}$, then (2.44) is a contraction mapping and Algorithm 3 converges to a minimum of (2.28) with a geometric rate.

Proof: Define the contraction mapping of Algorithm 3 as $T(\boldsymbol{\alpha}) \triangleq \frac{\rho \mathbf{f}(\boldsymbol{\alpha})}{\|\mathbf{f}(\boldsymbol{\alpha})\|_2}$. Then we have:

$$\|T(\boldsymbol{\alpha}) - T(\boldsymbol{\beta})\| = \left\| \frac{\|\mathbf{W}\mathbf{f}(\boldsymbol{\beta})\| \, \mathbf{f}(\boldsymbol{\alpha}) - \|\mathbf{W}\mathbf{f}(\boldsymbol{\alpha})\| \, \mathbf{f}(\boldsymbol{\beta})}{\|\mathbf{W}\mathbf{f}(\boldsymbol{\alpha})\| \, \|\mathbf{W}\mathbf{f}(\boldsymbol{\beta})\|} \right\| \tag{C.8}$$

$$\begin{aligned} &= \frac{\|(\mathbf{f}(\boldsymbol{\alpha}) - \mathbf{f}(\boldsymbol{\beta})) \, \|\mathbf{W}\mathbf{f}(\boldsymbol{\beta})\| + \mathbf{f}(\boldsymbol{\beta})((\|\mathbf{W}\mathbf{f}(\boldsymbol{\beta})\| - \|\mathbf{W}\mathbf{f}(\boldsymbol{\alpha})\|\|}{\|\mathbf{W}\mathbf{f}(\boldsymbol{\alpha})\| \, \|\mathbf{W}\mathbf{f}(\boldsymbol{\beta})\|} \\ &\leq \frac{\|\mathbf{W}\| \, \|\mathbf{f}(\boldsymbol{\beta})\| \, \|\mathbf{f}(\boldsymbol{\alpha}) - \mathbf{f}(\boldsymbol{\beta})\|}{\|\mathbf{W}\mathbf{f}(\boldsymbol{\alpha})\| \, \|\mathbf{W}\mathbf{f}(\boldsymbol{\beta})\|} \leq \frac{\kappa \, \|\mathbf{f}(\boldsymbol{\alpha}) - \mathbf{f}(\boldsymbol{\beta})\|}{\|\mathbf{W}\mathbf{f}(\boldsymbol{\alpha})\|} \end{aligned} \tag{C.9}$$

In Proposition A.26 of [41] it is shown that geometric convergence is assured when $\|T(\boldsymbol{\alpha}) - T(\boldsymbol{\beta})\| \leq \gamma \, \|\boldsymbol{\alpha} - \boldsymbol{\beta}\|$ with $\gamma < 1$. Then using (C.6) in (C.9) we arrive at (C.7) which satisfies the specified condition.

Bibliography

[1] N. Wiener, *The Extrapolation, Interpolation and Smoothing of Stationary Time Series.* New York: Wiley, 1949.

[2] S. M. Kay, *Fundamentals of Statistical Signal Processing: Estimation Theory.* Prentice-Hall, 1993.

[3] G. Golub and F. V. Loan, "An analysis of the total least squares problem," *SIAM J. Numer. Anal.*, vol. 17, pp. 883–893, Dec. 1980.

[4] A. Wiesel, Y. Eldar, and A. Yeredor, "Linear regression with gaussian model uncertainty: Algorithms and bounds," *IEEE Trans. Signal Process.*, vol. 56, pp. 2194–2205, June 2008.

[5] B. D. Moor, "Total least squares for affinely structured matrices and the noisy realization problem," *IEEE Trans. Signal Process.*, vol. 42, pp. 3104–3113, Nov. 1994.

[6] A. Pruessner and D. O'Leary, "Blind deconvolution using a regularized structured total least norm algorithm," *SIAM J. Mat. Anal. Appl.*, vol. 24, no. 4, pp. 1018–1037, 2002.

[7] P. Lemmerling, *Structured Total Least Squares: Analysis, Algorithms and Applications.* PhD thesis, Katholieke Universiteit Leuven, Leuven, May. 1999.

[8] Y. Eldar, A. Ben-Tal, and A. N. A. Beck, "Robust mean-squared error estimation in the presence of model uncertainties," *IEEE Trans. Signal Process.*, vol. 53, pp. 168–181, Jan 2005.

[9] A. Beck, Y. Eldar, and A. Ben-Tal, "Mean-squared error estimation for linear systems with block circulant uncertainty," *SIAM J. Mat. Anal. Appl.*, vol. 29, no. 3, pp. 712–730, 2007.

[10] L. El-Ghaoui and H. Lebret, "Robust solutions to least-squares problems with uncertain data," *SIAM J. Mat. Anal. Appl.*, vol. 18, no. 4, pp. 1035–1064, 1997.

[11] F. Alizadeh and D. Goldfarb, "Second-order cone programming," *Mathematical Programming*, vol. 95, pp. 1436–4646, Jan 2003.

[12] A. N. Tikhonov and V. Y. Arsenin, *Solution of Ill-Posed Problems.* V. H. Winston and Sons, 1977.

[13] A. Sayed and S. Chandrasekaran, "Parameter estimation with multiple sources and levels of uncertainties," *IEEE Trans. Signal Process.*, vol. 48, pp. 680–692, Mar 2000.

[14] M. Guillaud, *Transmission and Channel Modeling Techniques for Multiple-Antenna Communication Systems.* PhD thesis, TELECOM ParisTech., Paris, July. 2005.

[15] R. DeGroat and E. Dowling, "The data least squares problem and channel equalization," *IEEE Trans. Signal Process.*, vol. 42, pp. 407–411, May 1993.

[16] I. Markovsky, J. C. Willems, and S. V. Huffel, "Application of structured total least squares for system identification and model reduction," *IEEE Trans. Autom. Control*, vol. 50, pp. 1490–1500, Oct 2005.

[17] H. Chen, S. V. Huel, and D. V. Ormondt, "Application of the structured total least norm technique in spectral estimation," in *Proc. of the 8th European Signal Processing Conference*, 1996.

[18] J. Severson, *Modeling and Frequency Tracking of Marine Mammal Whistle Calls.* PhD thesis, Massachusetts Institute of Technology and Woods Hole Oceanographic Institution, Massachusetts, Feb. 2009.

[19] G. Golub and V. Pereyra, "The differentiation of pseudo-inverses and nonlinear least squares problems whose variables separate," *SIAM J. Numer. Anal.*, vol. 10, pp. 413–432, Apr. 1973.

[20] S. V. Huffel and J. Vandewalle, *The Total Least Squares Problem: Computational Aspects and Analysis.* Frontiers in Applied Mathematics. SIAM, 1991.

[21] I. Markovsky and S. V. Huffel, "Overview of total least-squares methods," *Signal Process.*, vol. 87, pp. 2283–2302, Oct 2007.

[22] A. Beck, A. Ben-Tal, and C. Kanzow, "A fast method for finding the global solution of the regularized structured total least squares problem for image deblurring," *SIAM J. Mat. Anal. Appl.*, vol. 30, pp. 419–443, Feb 2008.

[23] V. Z. Mesarovic, N. P. Galatsanos, and A. K. Katsaggelos, "Regularized constrained total least squares image restoration," *IEEE Trans. Image Process.*, vol. 4, pp. 1096–1109, 1995.

[24] T. Abatzoglou, J. Mendel, and G. Harada, "The constrained total least squares technique and its application to harmonic superresolution," *IEEE Trans. Signal Process.*, vol. 39, pp. 1070–1087, May 1991.

[25] M. Pilanci, O. Arikan, B. Oguz, and M. Pinar, "Structured least squares with bounded data uncertainties," in *IEEE Int. Conf. Acoust. Speech Sign. Processing (ICASSP)*, 2009.

[26] M. Pilanci, O. Arikan, B. Oguz, and M. Pinar, "A novel technique for a linear system of equations applied to channel equalization," in *Signal Processing and Communications Applications Conference, 2009. SIU 2009. IEEE 17th*, 2009.

[27] M. Pinar and O. Arikan, "On robust solutions to linear least squares problems affected by data uncertainty and implementation errors with application to stochastic signal modeling," *Linear Algebra Appl*, vol. 391, no. 1, pp. 223–243, 2004.

[28] S. Chandrasekaran, G. Golub, M. Gu, and A. Sayed, "An efficient algorithm for a bounded errors-in-variables model," *SIAM J. Mat. Anal. Appl.*, vol. 20, pp. 839–859, Oct 1999.

[29] S. Chandrasekaran, M. Gu, A. Sayed, and K. E. Schubert, "The degenerate bounded errors-in-variables model," *SIAM J. Mat. Anal. Appl.*, vol. 23, pp. 138–166, Oct 2001.

[30] K. E. Schubert, *A New Look at Robust Estimation and Identification.* PhD thesis, University of California, Santa Barbara, Santa Barbara, CA, Sept. 2003.

[31] A. Yeredor, "The extended least squares criterion: Minimization algorithms and applications," *IEEE Trans. Signal Process.*, vol. 49, pp. 74–86, Jan 2000.

[32] P. Lemmerling and B. D. Moor, "Misfit versus latency," *Automatica*, vol. 37, pp. 2057–2067, 2001.

[33] M. Hayes, *Statistical Digital Signal Processing and Modeling.* John Wiley & Sons, Inc., 1996.

[34] A. E. Hoerl and R. W. Kennard, "Ridge regression: Biased estimation for nonorthogonal problems," *Technometrics*, vol. 42, pp. 80–86, Sept 2000.

[35] Y. C. Eldar, "Rethinking biased estimation: Improving maximum likelihood and the cramer-rao bound," *Foundations and Trends in Signal Processing*, vol. 1, no. 4, pp. 305–449, 2008.

[36] J. Dieudonn, *Foundations of Modern Analysis.* Academic Press, New York, 1960.

[37] R. Gray, "Toeplitz and circulant matrices: A review.," tech. rep., Stanford Univ. Inform. Sys. Lab., 1977.

[38] G. H. Golub and C. F. V. Loan, *Matrix Computations.* Johns Hopkins Univ. Press, 1996.

[39] G. H. Golub and U. von Matt, "Quadratically constrained least squares and quadratic problems," *Numer. Math.*, vol. 59, pp. 561–580, Dec 1991.

[40] F. Sroubek, G. Cristobal, and J. Flusser, "Unified approach to superresolution and multichannel blind deconvolution," *IEEE Trans. Image Process.*, vol. 16, pp. 2322–2332, Sept 2007.

[41] D. P. Bertsekas, *Nonlinear Programming, 2nd edition.* Athena Scientific, 1995.

[42] J. Rosen, H. Park, and J. Glick, "Formulation and solution of structured total least norm problems for parameter estimation," *IEEE Trans. Signal Process.*, vol. 44, pp. 2464–2474, Oct 1996.

[43] R. Fletcher, *Practical Methods of Optimization, 2nd edition.* John Wiley and Sons, Inc, 1987.

[44] S. V. Huffel, H. Chen, C. Decanniere, and P. V. Hecke, "Algorithm for time-domain nmr data fitting based on total least squares," *J. Magn Reson.*, vol. 110, no. 2, pp. 228–237, 1994.

[45] I. Markovsky, S. V. Huffel, and R. Pintelon, "Software for structured total least squares estimation," *Dept. EE, K.U. Leuven, Tech. Rep. 03-136*, 2003.

[46] D. P. O'Leary, *Scientific computing with case studies.* SIAM Press, 2009.

[47] E. J. Candes and T. Tao, "Decoding by linear programming," *IEEE Trans. Inf. Theory*, vol. 51, pp. 4203–4215, Dec 2005.

[48] G. Pfander, H. Rauhut, and J. Tanner, "Identification of matrices having a sparse representation," *IEEE Trans. Signal Process.*, vol. 56, pp. 5376–5388, Nov 2008.

[49] M. Herman and T. Strohmer, "High-resolution radar via compressed sensing," *IEEE Trans. Signal Process.*, vol. 57, pp. 2275–2284, Jun 2009.

[50] E. J. Candes, "The restricted isometry property and its implications for compressed sensing," *C. R. Math.*, vol. 346, pp. 589–592, May 2008.

[51] V. Saligrama, "Deterministic designs with deterministic guarantees: Toeplitz compressed sensing matrices, sequence designs and system identification," *arXiv:0806.4958*, Jun 2008.

[52] W. Bajwa, J. Haupt, G. Raz, S. Wright, and R. Nowak, "Toeplitz-structured compressed sensing matrices," in *IEEE/SP 14th Workshop on Statistical Signal Processing, SSP 07, pp. 294-298, Aug, 2007.*

[53] E. J. Candes, J. Romberg, and T. Tao, "Stable signal recovery from incomplete and inaccurate measurements," *Comm. Pure Appl. Math.*, vol. 59, pp. 120–1223, Aug 2006.

[54] M. Herman and T. Strohmer, "General deviants: an analysis of perturbations in compressed sensing," *arXiv:0907.2955*, Feb 2009.

[55] G. W. Stewart, "On the perturbation of pseudo-inverses, projections and linear least squares problems," *SIAM Review*, vol. 19, pp. 634–662, Oct 1977.

[56] A. M. Bruckstein, D. L. Donoho, and M. Elad, "From sparse solutions of systems of equations to sparse modeling of signals and images," *Journal of Fourier Analysis and Applications*, vol. 51, pp. 34–81, Feb 2009.

[57] J. Tropp and A. Gilbert, "Signal recovery from random measurements via orthogonal matching pursuit," *IEEE Trans. Inf. Theory*, vol. 53, pp. 4655–4666, Dec 1977.

[58] M. Pilanci, O. Arikan, and M. Pinar, "Structured least squares problems and robust estimators," *IEEE Trans. Signal Process.*, vol. 58, pp. 2453–2465, May 2010.

[59] K. Yongdai and K. Jinseog, "Gradient lasso for feature selection," in *Proceedings of the twenty-first international conference on Machine learning, July, 2004.*

[60] W. Bajwa, A. Sayeed, and R. Nowak, "Sparse multipath channels: Modeling and estimation," in *Digital Signal Processing Workshop and 5th IEEE Signal Processing Education Workshop, pp. 320-325, 2008.*

[61] A. Stam, "Some inequalities satisfied by the quantities of information of fisher and shannon," *Information and Control*, vol. 2, no. 2, pp. 101–112, 1959.

[62] T. M. Cover and J. A. Thomas, *Elements of information theory.* John Wiley and Sons, 2006.

[63] E. Arikan, "Channel polarization: A method for constructing capacity-achieving codes for symmetric binary-input memoryless channels," *IEEE Trans. Inf. Theory*, vol. 2, no. 2, pp. 101–112, 2007.

[64] K. L. Chung, *A Course in Probability Theory.* 2nd ed. Academic: New York, 1974.

[65] L. Kozachenko and N. Leonenko, "Sample estimate of the entropy of a random vector," *Probl. Peredachi Inf.*, vol. 23, no. 2, pp. 9–16, 1987.

[66] E. v. Berg, M. P. Friedlander, G. Hennenfent, F. Herrmann, R. Saab, and Ö. Yılmaz, "Sparco: A testing framework for sparse reconstruction," Tech. Rep. TR-2007-20, Dept. Computer Science, University of British Columbia, Vancouver, October 2007.

[67] P. Stoica and T. L. Marzetta, "Parameter estimation problems with singular information matrices," *IEEE Trans. Signal Process.*, vol. 49, pp. 87–90, Jan 2001.

[68] H. Weyl, "Das asymptotische verteilungsgesetz der eigenwerte linearer partieller differentialgleichungen (mit einer anwendung auf die theorie der hohlraumstrahlung)," *Journal Mathematische Annalen*, vol. 71, pp. 441–479, Dec 1912.